



3 4456 0349806 1

CENTRAL RESEARCH LIBRARY
DOCUMENT COLLECTION

ORNL-1817

Chemistry-Radiation and
Radiochemistry

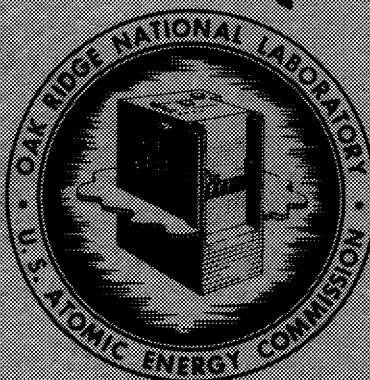
cy 4

DECLASSIFIEDPer Letter Instructions of
AEC LIST -9-1-SZH. Johnston

ORNL-1817-56

PRODUCTS PRODUCED IN CONTINUOUS
NEUTRON IRRADIATION OF THORIUMA. T. Gresky
E. D. ArnoldOAK RIDGE NATIONAL LABORATORY
CENTRAL RESEARCH LIBRARY
DOCUMENT COLLECTION**LIBRARY LOAN COPY**

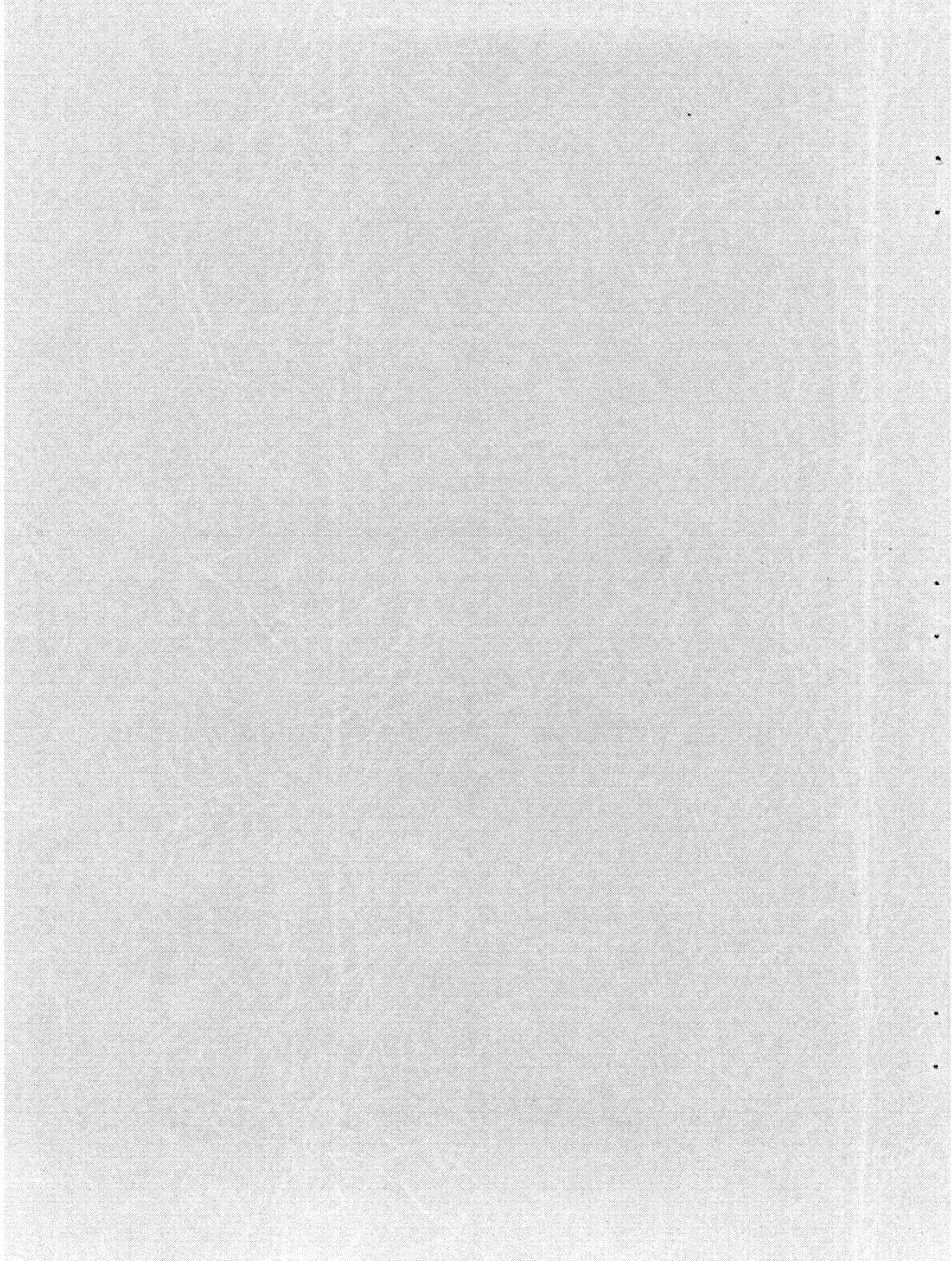
DO NOT TRANSFER TO ANOTHER PERSON

If you wish someone else to see this document,
send in name with document and the library will
arrange a loan.

OAK RIDGE NATIONAL LABORATORY
OPERATED BY
UNION CARBIDE NUCLEAR COMPANY
A Division of Union Carbide and Carbon Corporation



POST OFFICE BOX P - OAK RIDGE, TENNESSEE



ORNL-1817

Copy No. 4

Contract No. W-7405, eng 26

CHEMICAL TECHNOLOGY DIVISION

PRODUCTS PRODUCED IN CONTINUOUS NEUTRON

IRRADIATION OF THORIUM

A. T. Gresky

E. D. Arnold

DATE ISSUED

FEB 6 1956

OAK RIDGE NATIONAL LABORATORY
Operated by
UNION CARBIDE NUCLEAR COMPANY
A Division of
UNION CARBIDE AND CARBON CORPORATION
Post Office Box P
Oak Ridge, Tennessee

MARTIN MARIETTA ENERGY SYSTEMS LIBRARIES



3 4456 0349806 1

INTERNAL DISTRIBUTION

- | | |
|--|---|
| 1. C. E. Center | 34. C. E. Winters |
| 2. Biology Library | 35. D. W. Cardwell |
| 3. Health Physics Library | 36. E. M. King |
| 4-5. Central Research Library | 37. W. K. Eister |
| 6. Reactor Experimental
Engineering Library | 38. F. R. Bruce |
| 7-12. Laboratory Records Department | 39. D. E. Ferguson |
| 13. Laboratory Records, ORNL R.C. | 40. H. K. Jackson |
| 14. A. M. Weinberg | 41. H. E. Goeller |
| 15. L. B. Emlet (K-25) | 42. D. D. Cowen |
| 16. J. P. Murray (Y-12) | 43. R. A. Charpie |
| 17. E. H. Taylor | 44. J. A. Lane |
| 18. E. D. Shipley | 45. M. J. Skinner |
| 19-20. F. L. Culler | 46. R. E. Blanco |
| 21. F. C. VonderLage | 47. G. E. Boyd |
| 22. W. H. Jordan | 48. W. E. Unger |
| 23. C. P. Keim | 49. R. R. Dickison |
| 24. J. H. Frye, Jr. | 50. R. B. Briggs |
| 25. S. C. Lind | 51. B. F. Bottenfield |
| 26. A. H. Snell | 52. Sigfred Peterson |
| 27. A. Hollaender | 53. W. C. Moore |
| 28. M. T. Kelley | 54. E. M. Shank |
| 29. K. Z. Morgan | 55. R. W. Stoughton |
| 30. T. A. Lincoln | 56. E. D. Arnold |
| 31. R. S. Livingston | 57. A. T. Gresky |
| 32. A. S. Householder | 58-60. ORNL - Y-12 Technical Library,
Document Reference Section |
| 33. C. S. Harrill | 61. J. A. Swartout |

EXTERNAL DISTRIBUTION

- | |
|--|
| 62. AF Plant Representative, Burbank |
| 63. AF Plant Representative, Marietta |
| 64-65. AF Plant Representative, Seattle |
| 66. AF Plant Representative, Wood-Ridge |
| 67. Alco Products, Inc. |
| 68-71. Argonne National Laboratory |
| 72. Armed Forces Special Weapons Project (Sandia) |
| 73. Armed Forces Special Weapons Project, Washington |
| 74-75. Army Chemical Center |
| 76-77. Atomic Energy Commission, Washington |
| 78. Battelle Memorial Institute |
| 79-80. Bettis Plant (WAPD) |
| 81-82. Brookhaven National Laboratory |
| 83. Bureau of Ships |
| 84. Chicago Patent Group |

- 85. Combustion Engineering, Inc. (CERD)
- 86. Dow Chemical Company (Rocky Flats)
- 87-90. duPont Company, Aiken
- 91. Foster Wheeler Corporation
- 92-94. General Electric Company (ANPD)
- 95-98. General Electric Company, Richland
- 99-100. Goodyear Atomic Corporation
- 101. Hanford Operations Office
- 102. Headquarters, Air Force Special Weapons Center
- 103. Iowa State College
- 104-106. Knolls Atomic Power Laboratory
- 107-108. Los Alamos Scientific Laboratory
- 109. Massachusetts Institute of Technology (Evans)
- 110. Materials Laboratory (WADC)
- 111. Mound Laboratory
- 112. National Advisory Committee for Aeronautics, Cleveland
- 113. National Bureau of Standards
- 114. National Lead Company of Ohio
- 115. Naval Medical Research Institute
- 116. Naval Research Laboratory
- 117. New Brunswick Area Office
- 118-119. New York Operations Office
- 120-121. North American Aviation, Inc.
- 122. Nuclear Metals, Inc.
- 123. Office of the Quartermaster General
- 124. Patent Branch, Washington
- 125-128. Phillips Petroleum Company (NRTS)
- 129. Pratt & Whitney Aircraft Division (Fox Project)
- 130. Public Health Service
- 131. Sylvania Electric Products, Inc.
- 132. Union Carbide Nuclear Company (C-31 Plant)
- 133-134. Union Carbide Nuclear Company (K-25 Plant)
- 135. USAF Project Rand
- 136. U. S. Naval Radiological Defense Laboratory
- 137. UCLA Medical Research Laboratory
- 138-139. University of California Radiation Laboratory, Berkeley
- 140-141. University of California Radiation Laboratory, Livermore
- 142. University of Rochester
- 143. Vitro Engineering Division
- 144-145. Western Reserve University (Friedell)
- 146. Wright Air Development Center (WCOSI-3)
- 147-261. Technical Information Extension (Oak Ridge)
- 262. Division of Research and Development, AEC, ORO

CONTENTS

	Page
0.0 Abstract	1
1.0 Introduction	1
2.0 Plotted Data	3
3.0 Formation of ^{232}U from ^{232}Th	21
3.1 Comparison of ^{232}U Content with that Produced during Batch Irradiation	31
4.0 Production and Decay of ^{234}Th	32
5.0 Effect of Irradiation Products on Neutron Economy	32
6.0 Importance of Ruthenium and the Ba^{140} - La^{140} Chain	43
7.0 Calculations of Irradiation Product Concentrations	55
8.0 Constants and Definitions of Symbols	60
9.0 References	62

O.O ABSTRACT

Calculated data and graphs describing the effects of continuous thermal-neutron irradiation of thorium, the usual method of operation of homogeneous reactors, are presented. The buildup and decay of U^{233} , Pa^{233} , other heavy isotopes, and fission products are considered on the basis of best available cross-section and fission-yield data. The effects of the heavy isotopes and fission products on neutron economy are discussed.

1.0 INTRODUCTION

This report discusses the amounts of various products formed by continuous irradiation of Th^{232} with different neutron fluxes at equilibrium, the condition that prevails in continuously processed thorium blankets surrounding homogeneous breeder reactors. The effects of these isotopes and their decay characteristics on neutron economy, breeding gains, and time cycles of chemical processing to remove high-cross-section isotopes are indicated. Special consideration is given to the products that introduce serious problems in chemical processing of the homogeneous reactor blanket, namely, U^{232} , Th^{234} , Ru^{103} , Ru^{106} , and Ba^{140} - La^{140} .

Pa^{233} , with a capture cross section of 150 b, U^{234} with one of 70 b, and the high-cross-section fission products constitute the primary obstacles to high breeding gains (see Fig. 1). Currently conceived chemical processes do not promise continuous removal of these materials from the blanket system, and it is therefore important to determine the optimum flux and blanket processing period. Since unit costs in U^{233} recovery by the Thorex process are inversely proportional to the g/t level,* it is also important to define the economic relations between neutron capture and chemical processing costs. However, this can be done only by a complete cost analysis.

* The "g/t level" is defined as the grams of $Pa^{233} + U^{233}$ per ton of thorium.

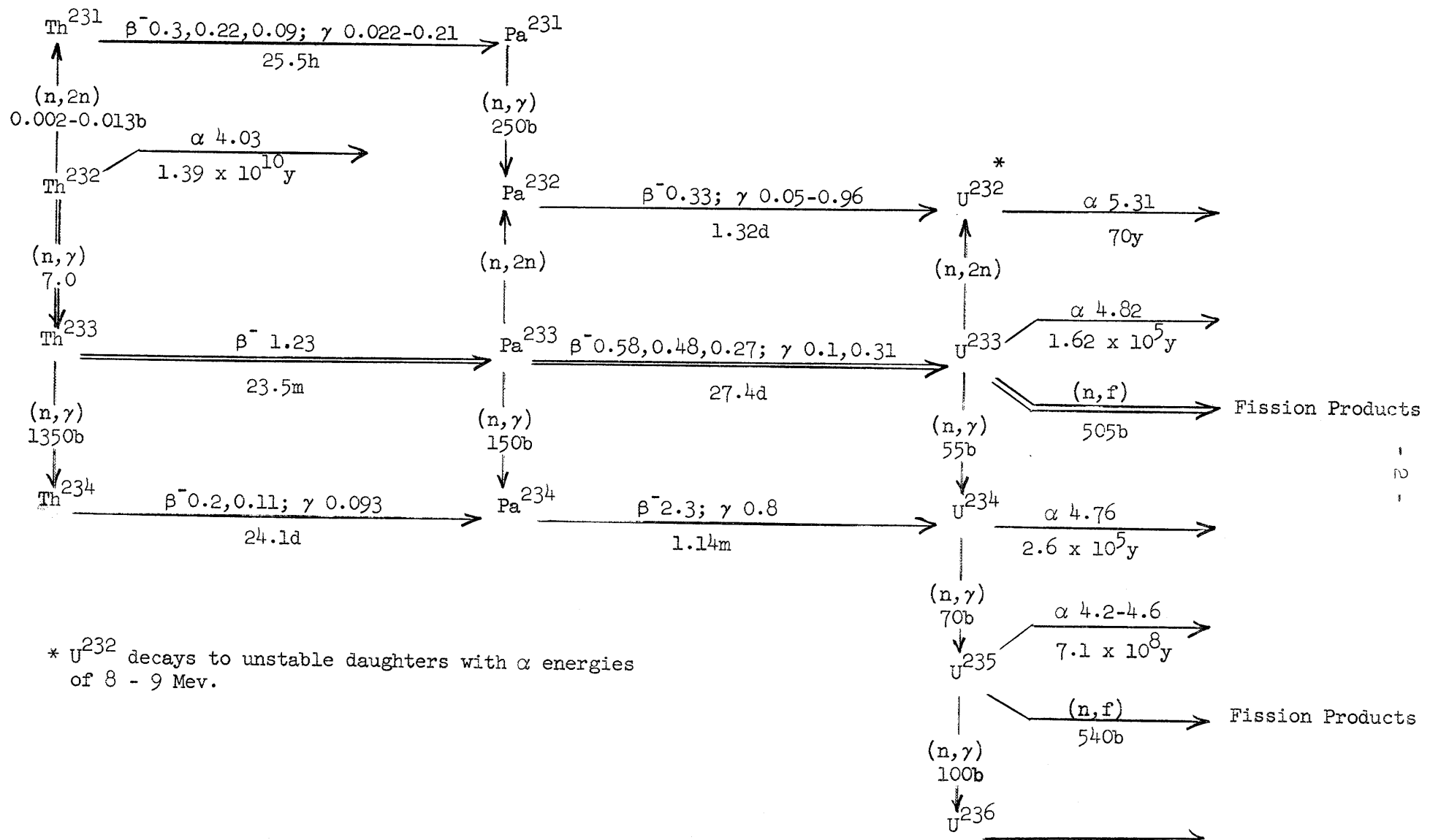


Fig. 1. NUCLEAR REACTIONS THAT OCCUR WHEN Th^{232} IS IRRADIATED WITH THERMAL NEUTRONS.
CROSS-SECTION DATA WERE OBTAINED FROM REFERENCES 1, 2, AND 3.

Since U^{233} of high isotopic purity can be obtained by isolating its parent, Pa^{233} , and subsequently allowing the Pa^{233} to decay, consideration should be given to separation of these isotopes by chemical processing of a thorium blanket after irradiation and/or decay periods at which the Pa^{233}/U^{233} ratio is about 0.2/1. It is somewhat fortuitous that this is also the ratio for optimum inventory economy in chemical processing schedules based on such factors, as costs of fissionable material inventories, shielding, and storage of thorium products.

2.0 PLOTTED DATA

Fig. 2: Summary plot showing the amounts of various isotopes as a function of blanket processing period, flux, and g/t level. This figure should be compared with a similar figure for batch operation⁴ to show the relative effects created by the two types of irradiation. When irradiation is continuous, there is a high concentration of the fissionable U^{233} throughout the irradiation period, in contrast to the gradually increasing U^{233} concentration when the concentration of all products is initially zero and increases exponentially. Therefore the concentrations of fission products and uranium isotopes other than U^{233} are generally higher in the equilibrium case by factors of 2-4. The ratio of total irradiation products to total mass 233 is 5-30% higher and the Pa^{233}/U^{233} ratio is slightly lower in the equilibrium case. The Th^{234} is essentially the same in the two cases. Conclusions from a study of these relative effects are that the equilibrium case permits greater contamination of the U^{233} product by the undesirable U^{232} and U^{234} isotopes and necessitates conditions requiring greater fission product decontamination in the chemical processing cycles.

Fig. 3: Summary plot showing the extraneous neutron captures by Pa^{233} , U^{234} , and fission products as a function of flux, processing period, and g/t level. The total capture of neutrons by isotopes other than Th^{232} increases by a factor of about 2 with a 10-fold increase in flux. However, capture by fission products decreases by a factor of about 2.5 owing to the lowering of the U^{233} concentration. The very significant increase in Pa^{233} captures is a result of both its 150-b cross section and the sharply increasing Pa^{233} equilibrium concentrations at the higher fluxes. From this

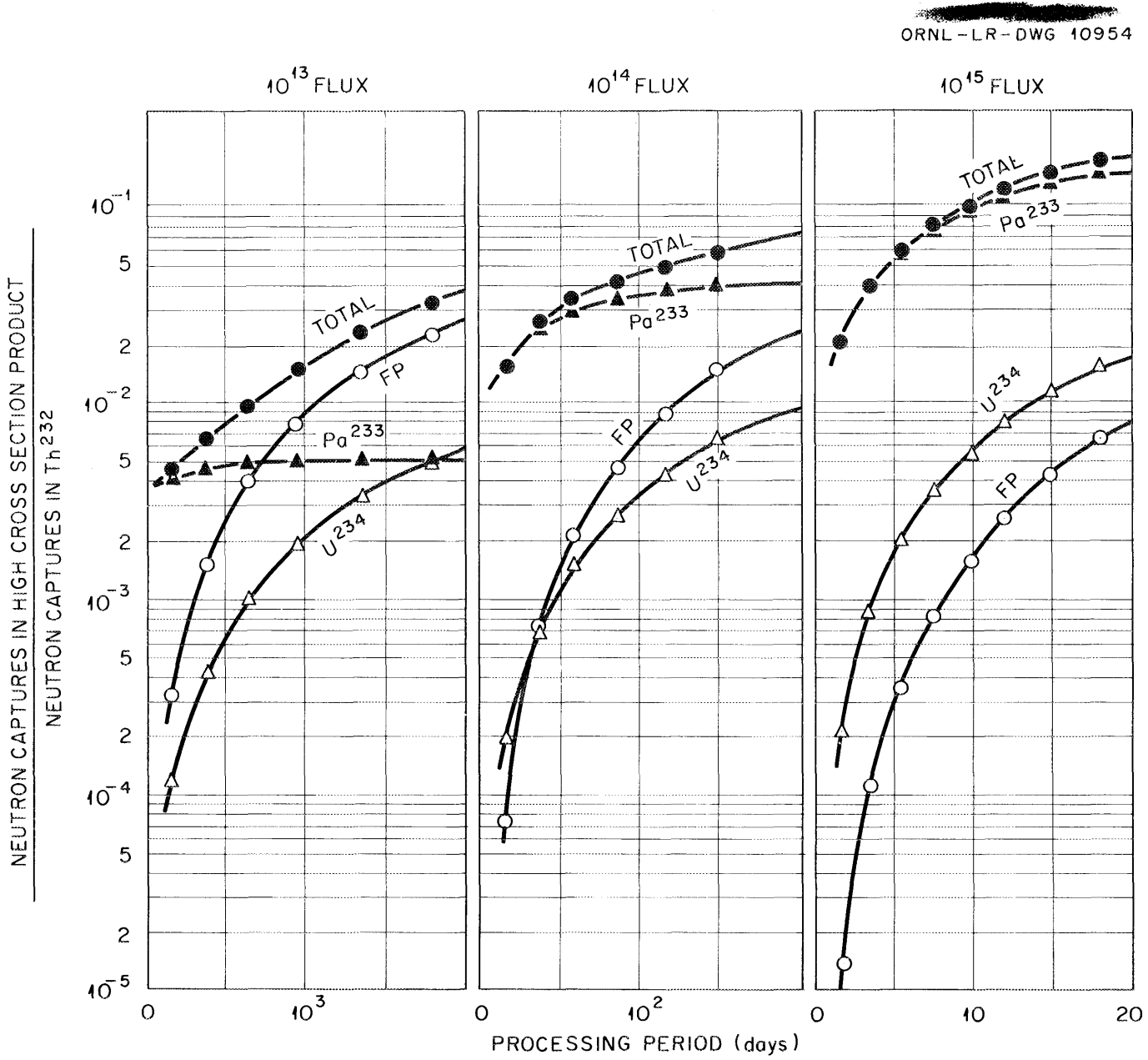


Fig. 2. Effect of Blanket Processing Period, Flux, and g/t Level on Extraneous Neutron Capture by Products Formed in Irradiation of Th^{232} . Points on line correspond to 1000 g/t, 2000 g/t, etc.

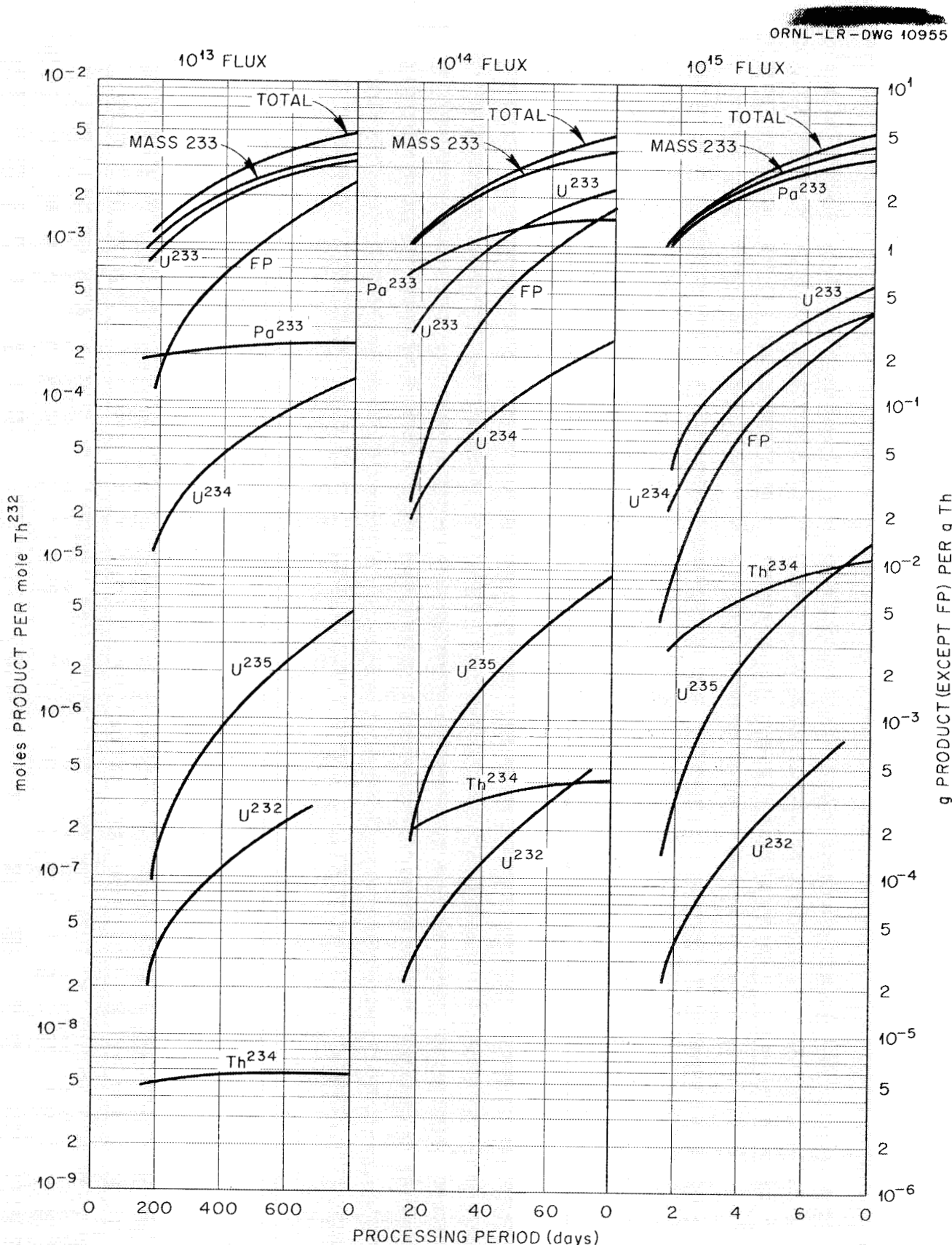


Fig. 3. Effect of Reactor Processing Period, Flux, and g/t Level on Products Formed in Irradiation of Th²³².

figure may be estimated the effect of Pa^{233} , fission products, and U^{234} on anticipated breeding gains at various fluxes. For example, a ratio of 0.3/1 on the ordinate would be equivalent to conditions which allow conversion only, so that the difference between 0.3/1 and the plotted values for total extraneous captures becomes an approximate measure of the number of neutrons that remain available for excess U^{233} production and/or losses by leakage, capture in reactor components, etc. These data indicate that the overall neutron economy will decrease with increasing flux and that Pa^{233} and the high-cross-section fission products are the controlling factors in extraneous neutron captures. If neutron losses to high-cross-section products of irradiation were the only consideration in the overall economy of power production, use of blanket fluxes greater than 10^{14} would be uneconomic.

Fig. 4-8: Plots showing concentrations of products formed in irradiation of Th^{232} as a function of flux and processing period. It may be seen that the concentration ratio of fission products to isotopes of mass 233 decreases with an increase in flux, while the fission product/ U^{234} concentration ratio increases slightly. Data are tabulated in Tables 1-5.

Fig. 9: Plot showing the effect of flux on the length of the processing or irradiation period necessary to obtain various values of mass 233 concentration (g/t level) in Th^{232} .

Fig. 10: Plot showing g/t level in irradiated thorium as a function of flux and processing period.

Figs. 11 and 12: Plots showing $\text{Pa}^{233}/\text{U}^{233}$ ratio as a function of flux and g/t level and of flux and decay time after discharge from reactor, respectively.

Figs. 13-15: Plots showing U^{232} concentrations and/or activities at time of discharge as a function of flux, processing period, and/or g/t level. The data are tabulated in Tables 6-8. The cross sections⁵ appearing on the plots are representative of the range of available data and are known to vary with neutron energy and/or reactor geometry.

Fig. 16: Plot showing the effects of storage time on buildup and decay of α activity due to U^{232} daughters.

Figs. 17 and 18: Plots showing Th^{234} concentration as a function of flux and g/t level and of decay time, respectively. The data indicate the decay time necessary to permit direct refabrication or metallurgy of thorium.

Table 1. Concentrations of Products Formed by Irradiation of Th²³² at Flux of 10¹³ n/cm²/sec

g Mass 233 per ton Th ²³²	Blanket Processing Rate (reactor vol/day)	Blanket Processing Period (days)	$\frac{N_{13}}{N_{O2_4} \times 10^4}$	$\frac{N_{23}}{N_{O2_4} \times 10^4}$	$\frac{N_{24}}{N_{O2_4} \times 10^4}$	$\frac{N_{25}}{N_{O2}}$	$\frac{N_{FP}}{N_{O2_4} \times 10^4}$	$\frac{N_{O4}}{N_{O2_4} \times 10^9}$	Total Products $\frac{N}{N_{O2_4} \times 10^4}$
1,000	5.659×10^{-3}	176.7	1.945	8.012	0.1106	1.075×10^{-7}	1.2355	4.827	10.69
2,000	2.592×10^{-3}	385.8	2.158	17.756	0.4235	8.124×10^{-7}	5.9778	5.299	23.33
3,000	1.5674×10^{-3}	638	2.240	27.631	0.9849	2.799×10^{-6}	15.3834	5.478	38.58
4,000	1.055×10^{-3}	947.8	2.284	37.544	1.8647	6.978×10^{-6}	31.0544	5.572	57.29
5,000	7.474×10^{-4}	1338	2.310	47.475	3.1630	1.462×10^{-5}	55.4303	5.631	80.81
7,000	3.959×10^{-4}	2526	2.342	67.357	7.6782	4.852×10^{-5}	148.4678	5.699	152.10
10,000	1.320×10^{-4}	7576	2.366	97.204	25.5884	2.232×10^{-4}	642.6068	5.751	448.70

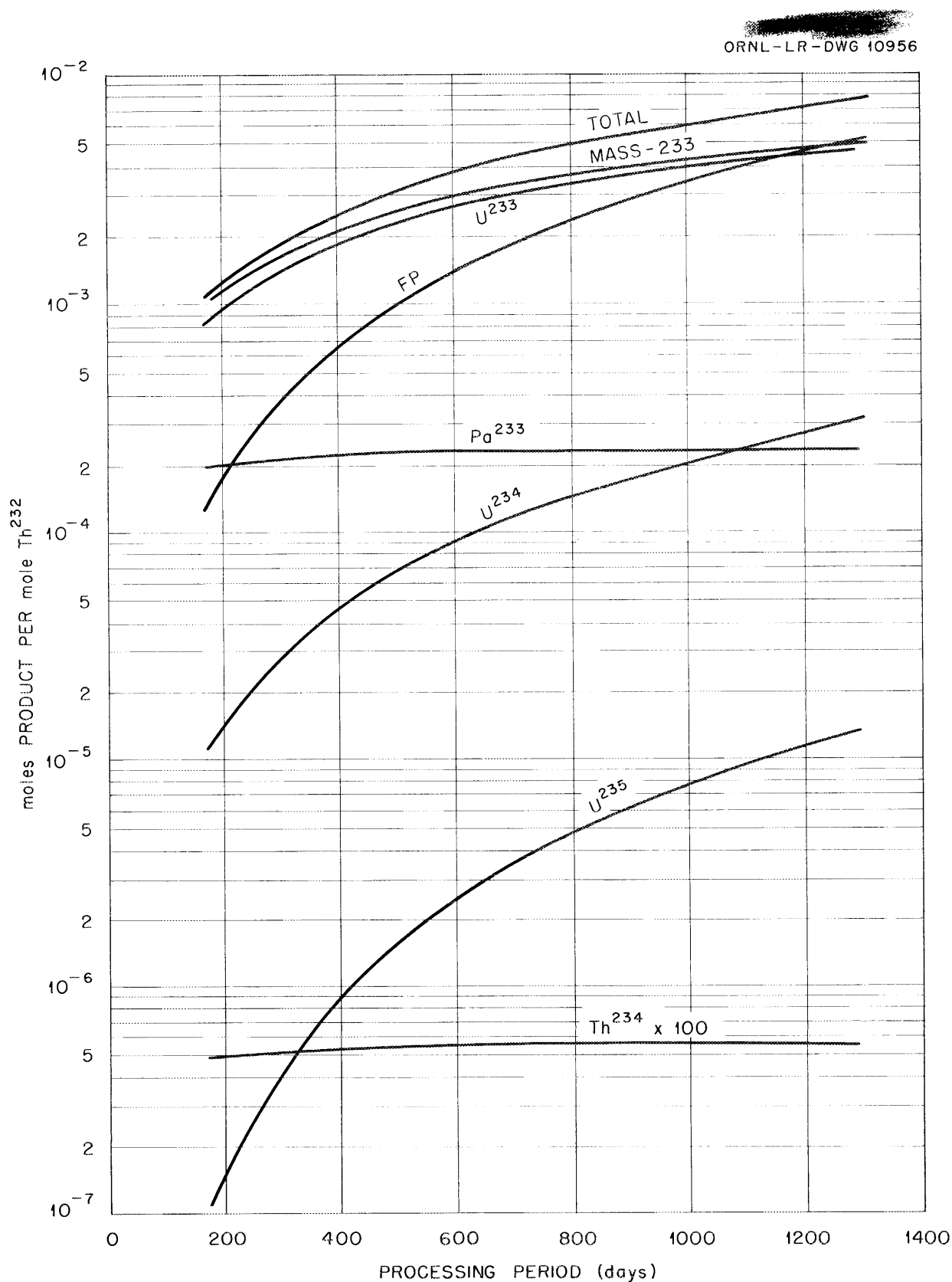


Fig. 4. Effect of Processing Period on Amounts of Various Products in Irradiated Th^{232} at a Thermal Flux of 10^{13} neutrons/cm 2 ·sec.

Table 2. Concentrations of Products Formed by Irradiation of Th^{232} at Flux of $5 \times 10^{13} \text{ n/cm}^2/\text{sec}$

g Mass Th^{232} per ton Th^{232}	Blanket Processing Rate (reactor vol/day)	Blanket Processing Period (days)	$\frac{N_{13}}{N_{\text{O}_2}}$ $\times 10^4$	$\frac{N_{23}}{N_{\text{O}_2}}$ $\times 10^4$	$\frac{N_{24}}{N_{\text{O}_2}}$ $\times 10^4$	$\frac{N_{25}}{N_{\text{O}_2}}$	$\frac{N_{\text{FP}}}{N_{\text{O}_2}}$ $\times 10^4$	$\frac{N_{\text{O}_4}}{N_{\text{O}_2}}$ $\times 10^7$	Total Products $\frac{N_{\text{O}_2}}{N_{\text{O}_2}}$ $\times 10^4$
1,000	2.893×10^{-2}	34.6	5.510	4.447	0.1583	1.509×10^{-7}	0.6707	0.719	10.4521
2,000	1.329×10^{-2}	75.2	7.707	12.207	0.5808	1.091×10^{-6}	4.0076	0.988	22.5095
3,000	8.227×10^{-3}	121.6	8.848	21.023	1.2578	3.448×10^{-6}	11.1496	1.123	36.7381
4,000	5.598×10^{-3}	178.6	9.586	30.242	2.2705	8.166×10^{-6}	23.5712	1.209	53.9658
5,000	4.013×10^{-3}	249.2	10.093	39.692	3.7001	1.641×10^{-5}	43.1558	1.267	75.2271
7,000	2.192×10^{-3}	456.2	10.746	58.953	8.4067	5.086×10^{-5}	117.3466	1.342	137.2876
10,000	8.188×10^{-4}	1221.3	11.298	88.272	25.2337	2.105×10^{-4}	470.3815	1.404	362.0992

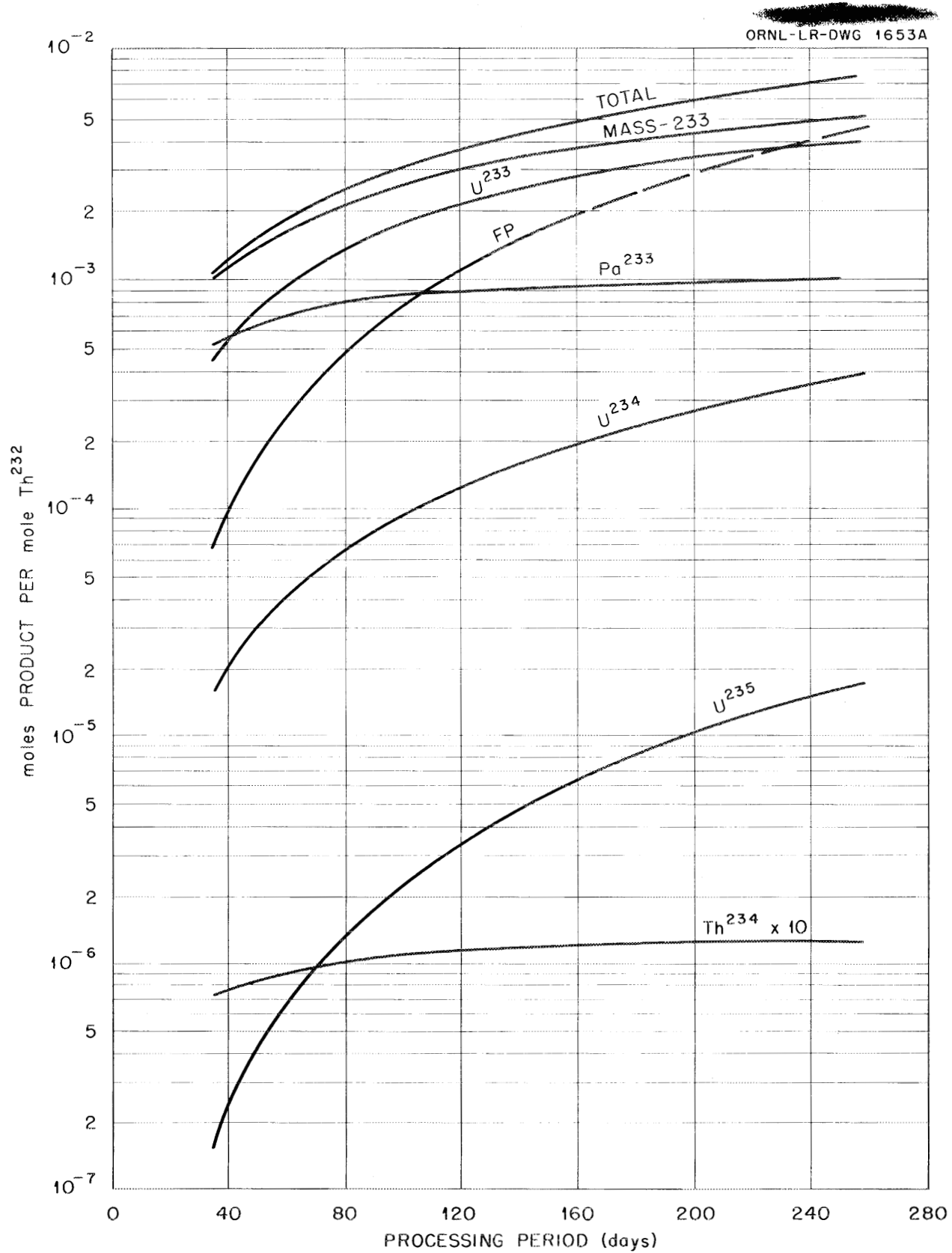


Fig. 5. Effect of Processing Period on Amounts of Various Products in Irradiated Th²³² at a Thermal Flux of 5×10^{13} neutrons/cm²·sec.

Table 3. Concentrations of Products Formed by Irradiation of Th^{232} at Flux of $10^{14} \text{ n/cm}^2/\text{sec}$

g Mass Th^{232} per ton Th^{232}	Blanket Processing Rate (reactor vol/day)	Blanket Processing Period (days)	$\frac{N_{13}}{N_{02_4}}$ $\times 10$	$\frac{N_{23}}{N_{02_4}}$ $\times 10$	$\frac{N_{24}}{N_{02_4}}$ $\times 10$	$\frac{N_{25}}{N_{02}}$	$\frac{N_{FP}}{N_{02_4}}$ $\times 10$	$\frac{N_{04}}{N_{02_4}}$ $\times 10^7$	Total Products $\frac{N_{02_4}}{x 10}$
1,000	5.843×10^{-2}	17.11	7.113	2.844	0.1922	1.816×10^{-7}	0.2832	1.904	10.2945
2,000	2.752×10^{-2}	36.34	11.176	8.738	0.6622	1.210×10^{-6}	2.7707	2.950	21.9770
3,000	1.705×10^{-2}	58.65	13.857	16.014	1.4482	3.866×10^{-6}	8.1962	3.625	35.4596
4,000	1.175×10^{-2}	85.11	15.772	24.056	2.5797	8.987×10^{-6}	17.8657	4.099	51.4345
5,000	8.535×10^{-3}	117.2	17.216	32.569	4.1344	1.767×10^{-5}	33.2994	4.453	70.7504
7,000	4.8175×10^{-3}	207.6	19.253	50.446	9.0224	5.232×10^{-5}	91.3777	4.946	124.9383
10,000	1.988×10^{-3}	503	21.159	78.411	24.9452	1.985×10^{-4}	344.188	5.400	298.5993

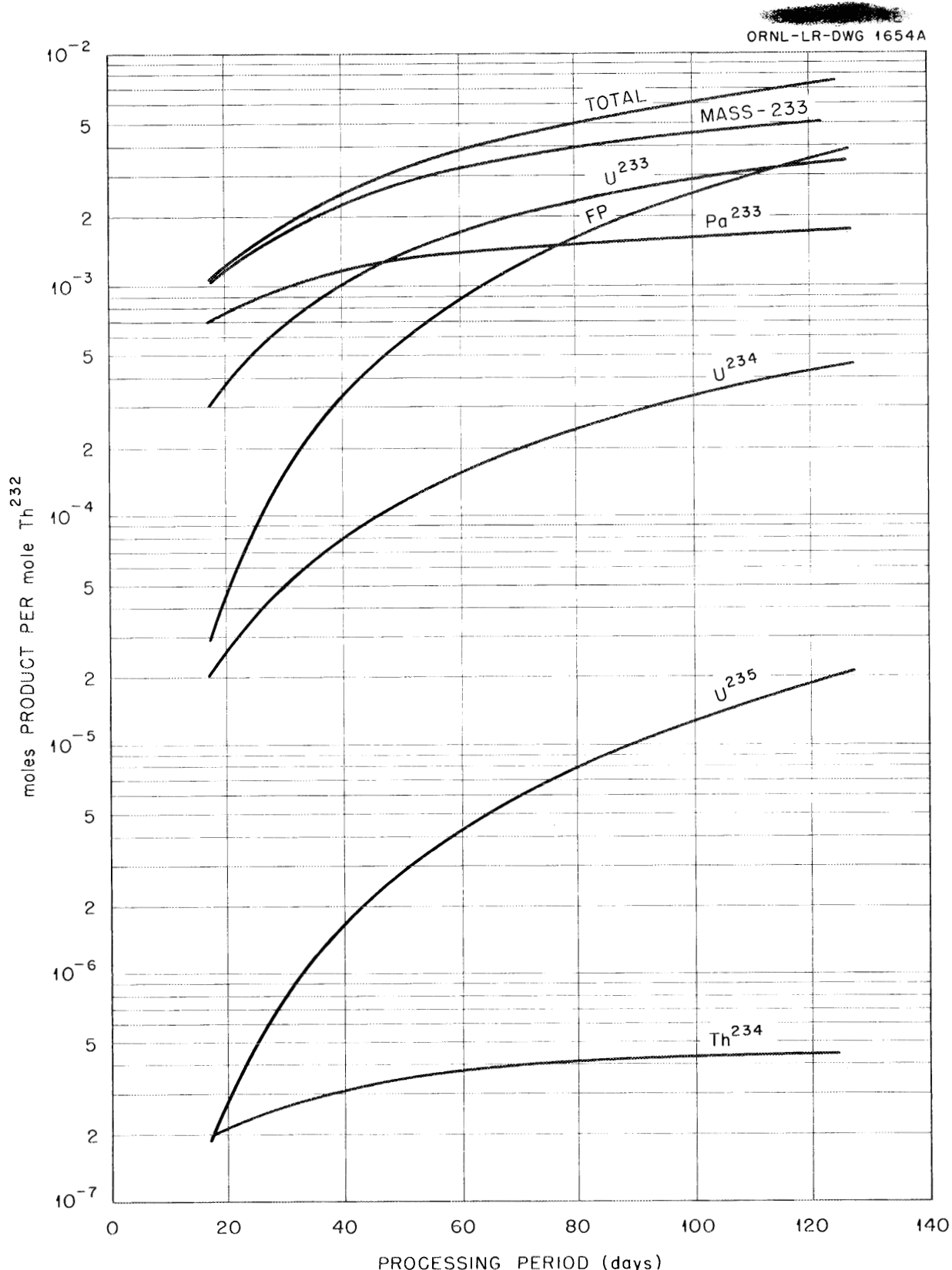


Fig. 6. Effect of Processing Period on Amounts of Various Products in Irradiated Th²³² at a Thermal Flux of 10^{14} neutrons/cm² · sec.

Table 4. Concentrations of Products Formed by Irradiation of Th^{232} at Flux of $5 \times 10^{14} \text{ n/cm}^2/\text{sec}$

g Mass Th^{232} per ton Th^{232}	Blanket Processing Rate (reactor vol/day)	Blanket Processing Period (days)	$\frac{N_{13}}{N_{\text{O}_2} \cdot 10^4}$	$\frac{N_{23}}{N_{\text{O}_2} \cdot 10^4}$	$\frac{N_{24}}{N_{\text{O}_2} \cdot 10^4}$	$\frac{N_{25}}{N_{\text{O}_2}}$	$\frac{N_{\text{FP}}}{N_{\text{O}_2} \cdot 10^4}$	$\frac{N_{04}}{N_{\text{O}_2} \cdot 10^7}$	Total Products $\frac{N_{\text{O}_2}}{\text{ton}} \cdot 10^4$
1,000	0.2959	3.38	9.228	0.729	0.2058	1.922×10^{-7}	0.1075	1.275	10.2311
2,000	0.143	6.99	17.302	2.612	0.8103	1.433×10^{-6}	0.7970	2.411	21.1612
3,000	9.158×10^{-2}	10.92	24.514	5.357	1.8136	4.585×10^{-6}	2.5523	3.441	33.0410
4,000	6.555×10^{-2}	15.25	31.070	8.758	3.2394	1.047×10^{-5}	5.8296	4.391	46.1308
5,000	4.975×10^{-2}	20.10	37.091	12.694	5.1257	1.992×10^{-5}	11.1330	5.274	60.7291
7,000	3.136×10^{-2}	31.89	47.894	21.805	10.5325	5.360×10^{-5}	30.3379	6.888	96.0053
10,000	1.717×10^{-2}	58.24	61.777	37.793	24.2689	1.622×10^{-4}	96.0387	9.016	173.5709

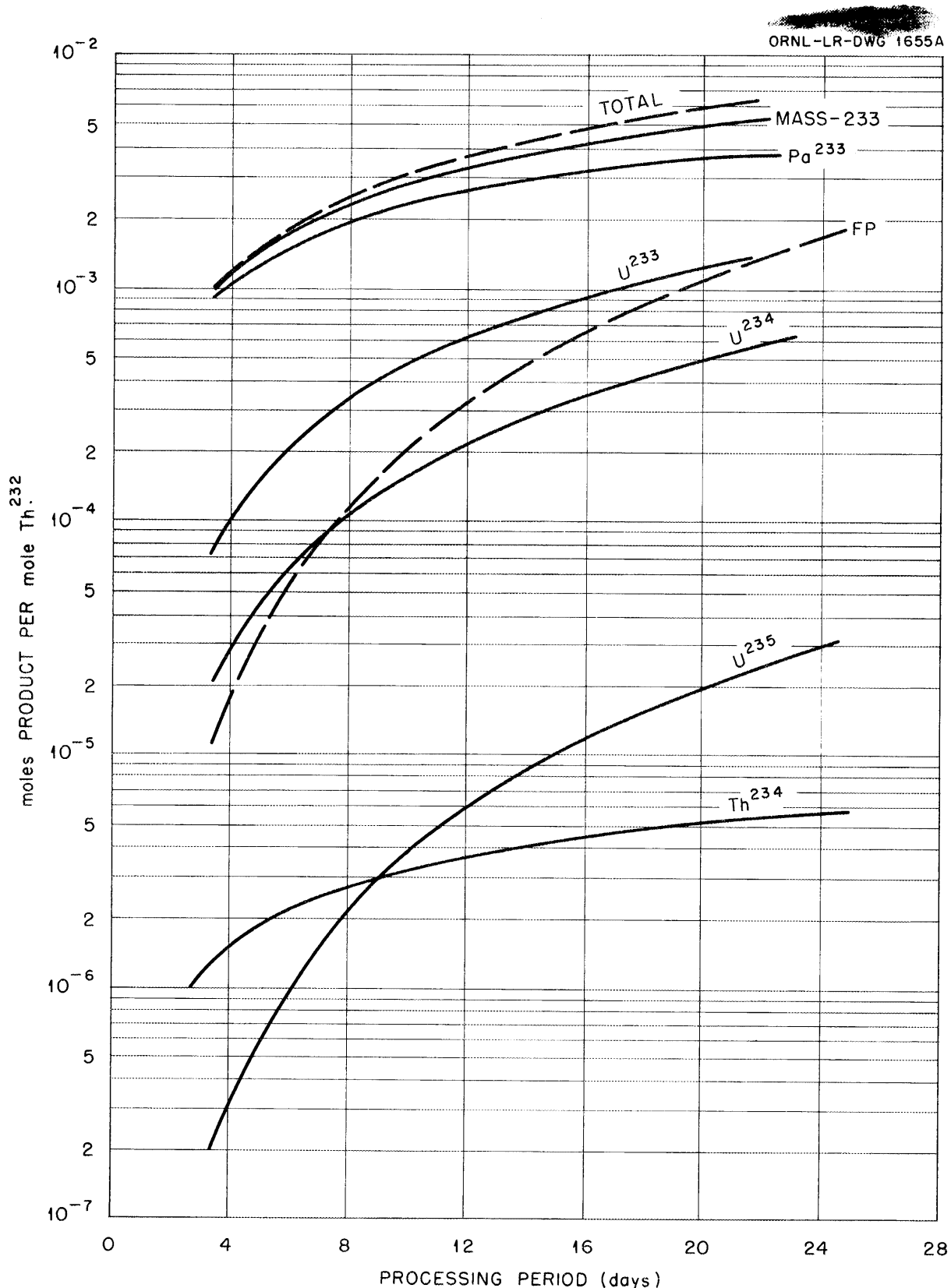


Fig. 7. Effect of Processing Period on Amounts of Various Products in Irradiated Th^{232} at a Thermal Flux of 5×10^{14} neutrons/cm 2 · sec.

Table 5. Concentrations of Products Formed by Irradiation of Th²³² at Flux of 10¹⁵ n/cm²/sec

g Mass 233 per ton Th ²³²	Blanket Processing Rate (reactor vol/day)	Blanket Processing Period (days)	$\frac{N_{13}}{N_{O2_4}} \times 10^4$	$\frac{N_{23}}{N_{O2_4}} \times 10^4$	$\frac{N_{24}}{N_{O2_4}} \times 10^4$	$\frac{N_{25}}{N_{O2}} \times 10^4$	$\frac{N_{FP}}{N_{O2_4}} \times 10^4$	$\frac{N_{O4}}{N_{O2_5}} \times 10^5$	Total Products $\frac{N_{O2_4}}{N_{O2_4}} \times 10^4$
1,000	0.5931	1.69	9.579	0.378	0.2102	1.958×10^{-7}	0.0556	0.266	10.2236
2,000	0.2883	3.47	18.520	1.394	0.8379	1.472×10^{-6}	0.4219	0.521	20.9776
3,000	0.1861	5.37	26.957	2.914	1.8902	4.720×10^{-6}	1.3664	0.769	32.5685
4,000	0.1346	7.43	34.988	4.840	3.3874	1.074×10^{-5}	3.1378	1.011	44.9928
5,000	0.1035	9.66	42.664	7.121	5.3561	2.030×10^{-5}	6.0039	1.249	58.4709
7,000	6.746×10^{-2}	14.82	57.208	12.491	10.8934	5.331×10^{-5}	16.1579	1.717	89.3761
10,000	3.989×10^{-2}	25.1	77.390	22.180	24.1266	1.520×10^{-4}	48.5213	2.406	149.7176

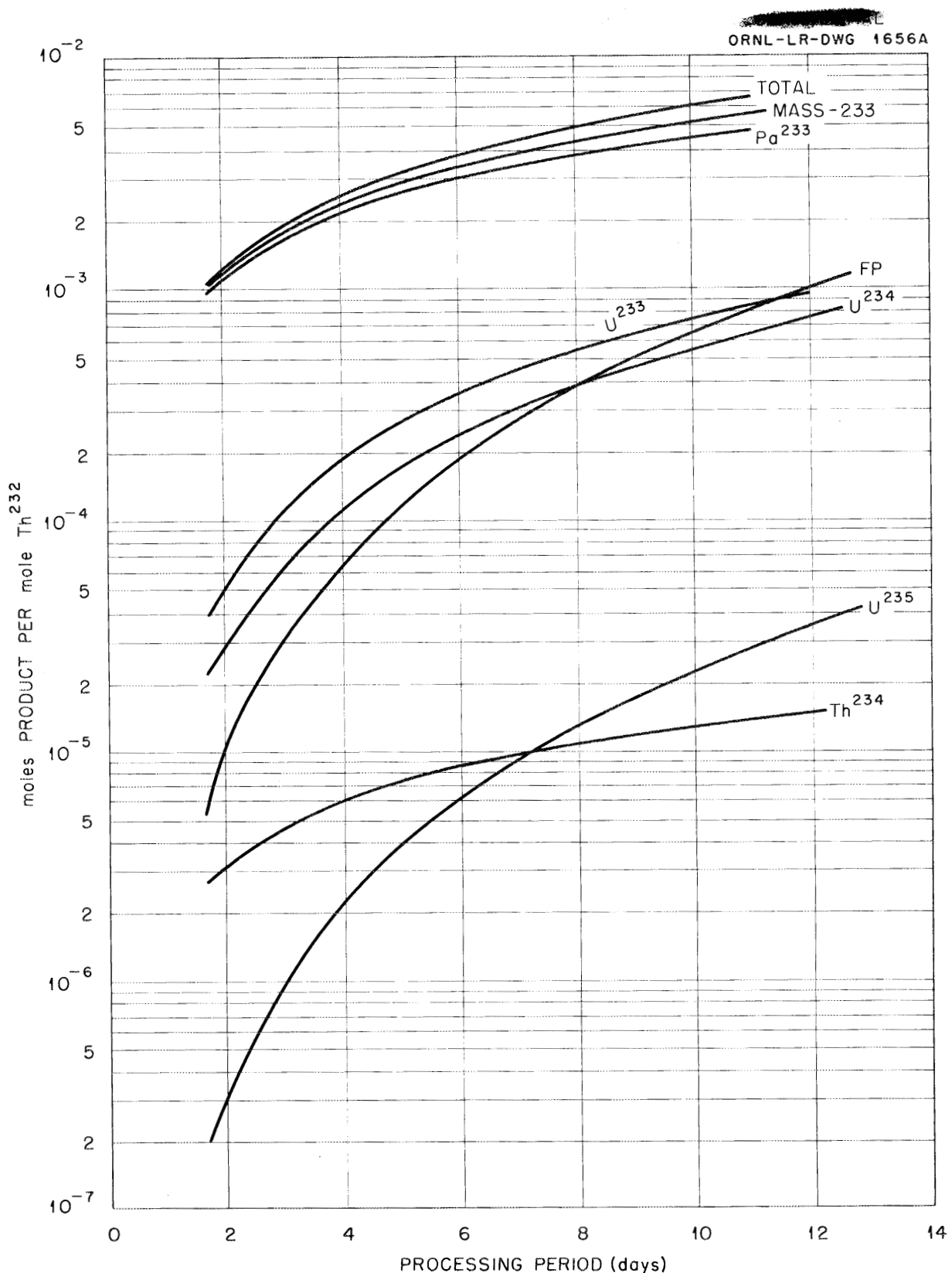


Fig. 8. Effect of Processing Period on Amounts of Various Products in Irradiated Th^{232} at a Thermal Flux of 10^{15} neutrons/cm 2 ·sec.

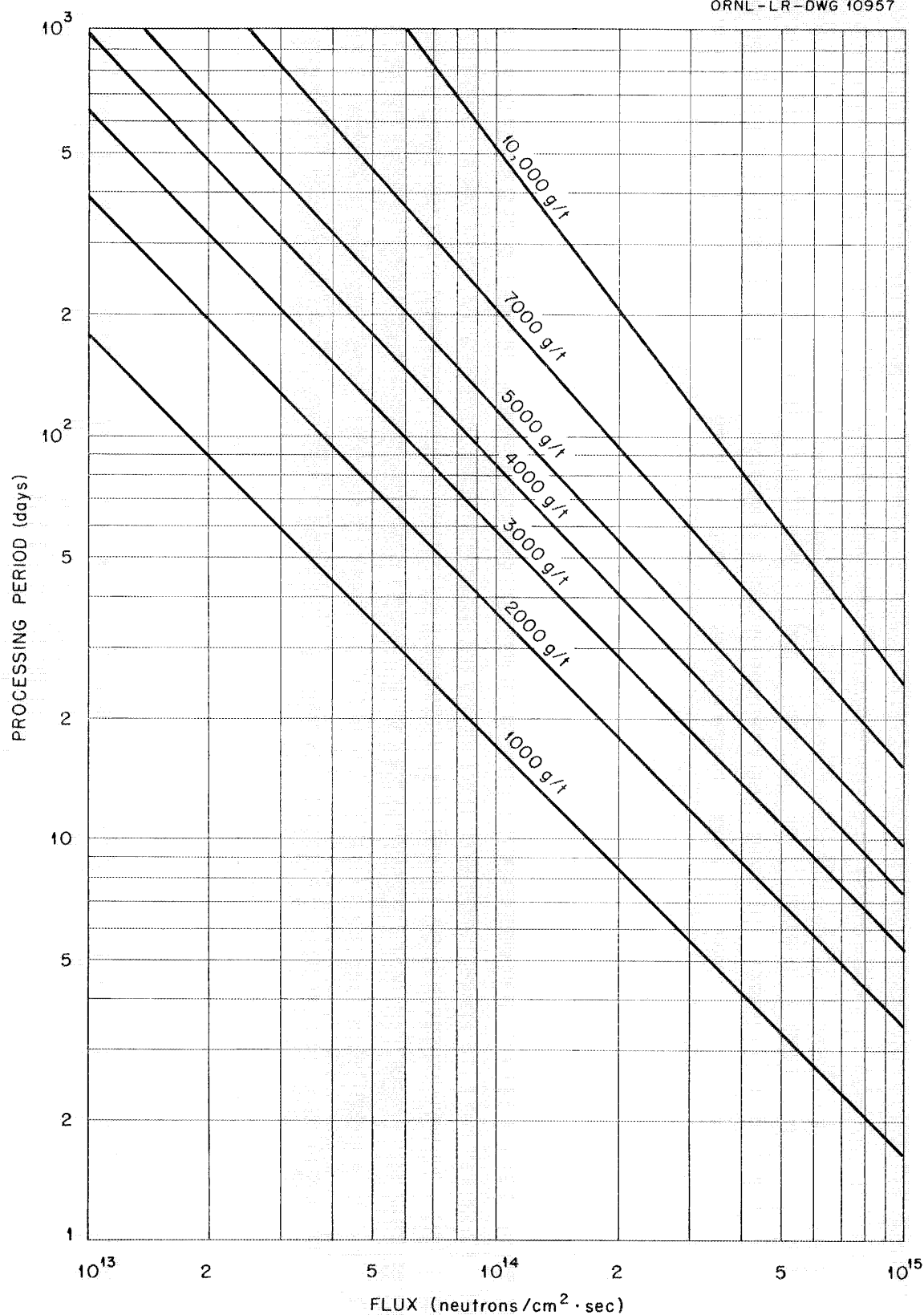


Fig. 9. Effect of Flux and Processing Period on Production of Isotopes of Mass-233.

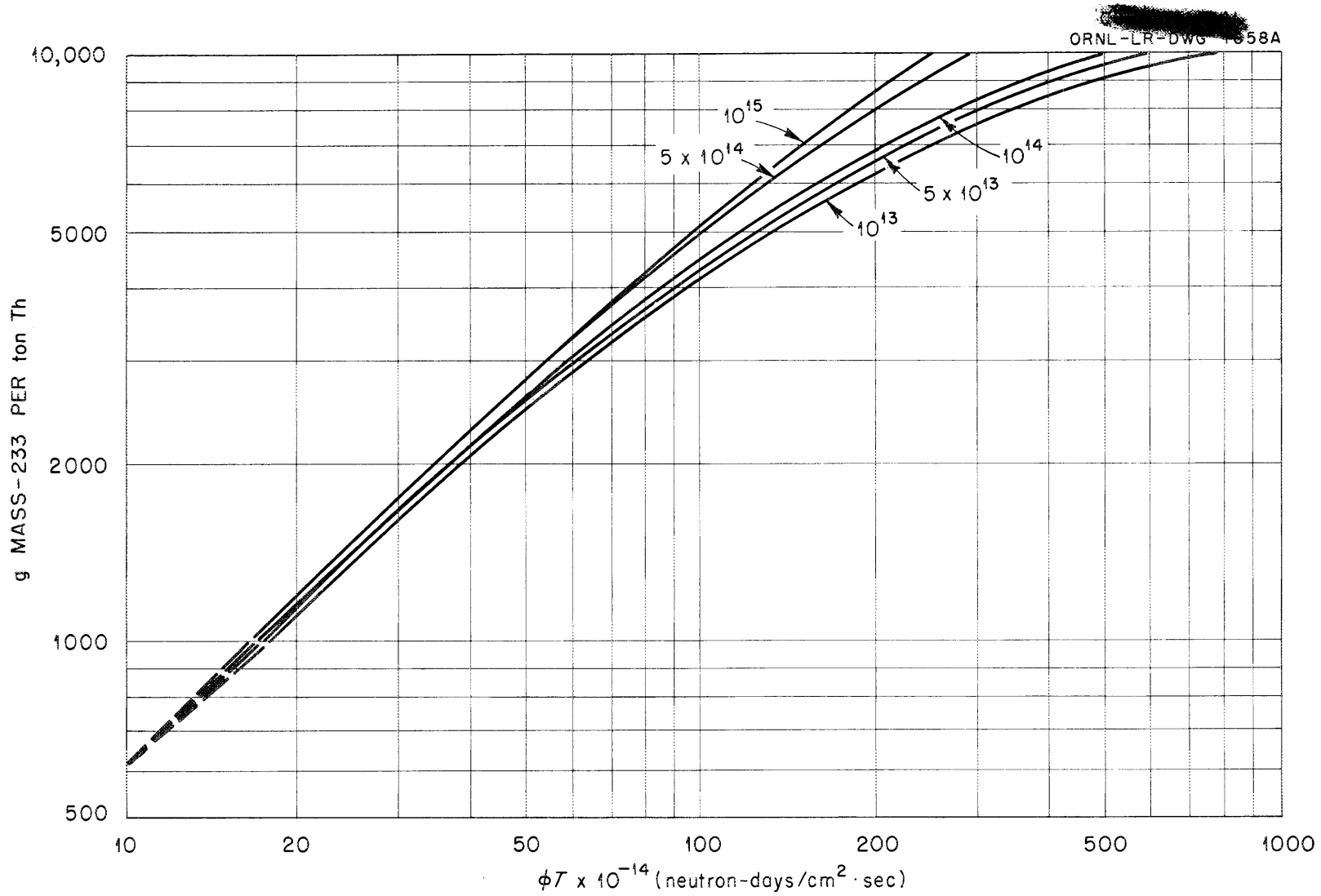


Fig. 10. Effect of Flux and Processing Period on g/t Level.

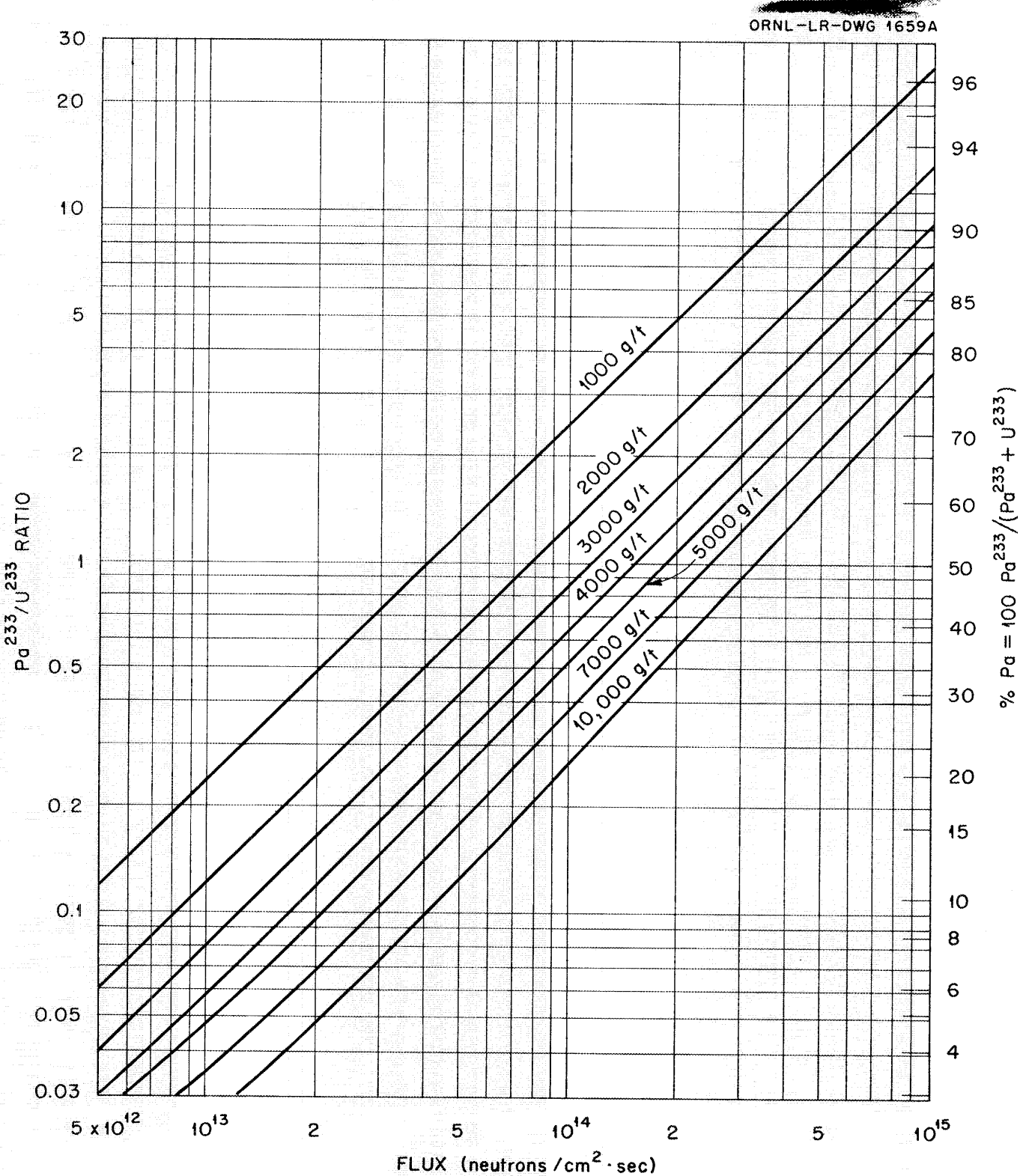


Fig. 11. Effect of Flux and g/t Level on $\text{Pa}^{233}/\text{U}^{233}$ Ratio.

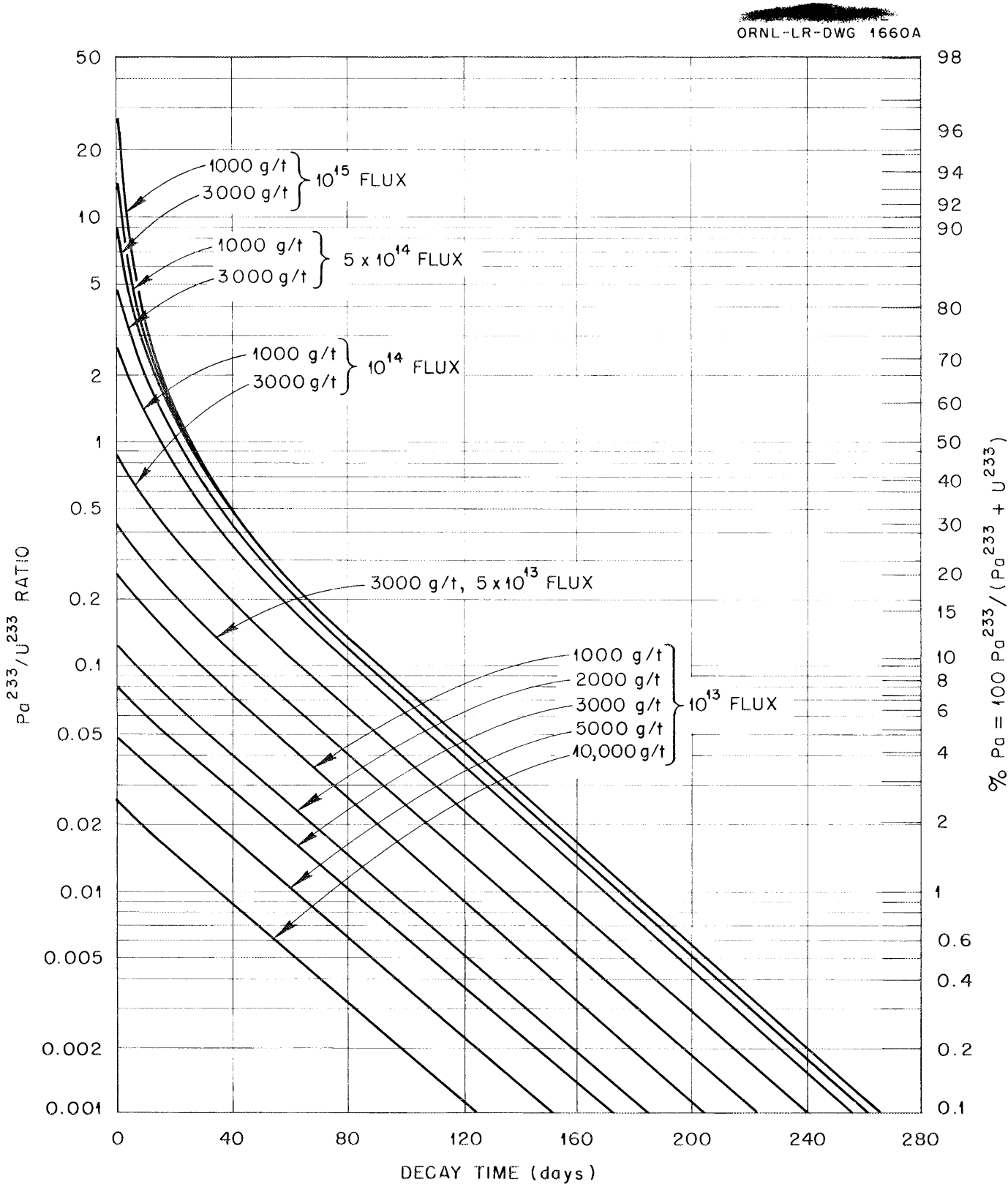


Fig. 12. Effect of Flux, g/t Level, and Decay Time After Removal from Reactor
on $\text{Pa}^{233}/\text{U}^{233}$ Ratio.

Figs. 19-23: Plots showing extraneous neutron captures as a function of the length of the processing period at various fluxes and g/t levels. It may be seen that the losses to Pa^{233} increase with flux and g/t level while losses to fission products increase with g/t level but decrease with flux. The loss to U^{234} increases only slightly with flux. The data are tabulated in Table 8.

Fig. 24: Composite plot showing extraneous neutron captures as a function of flux, g/t level, and processing period.

Figs. 25 and 26: Plots showing Ru^{103} and Ru^{106} activities at time of discharge as a function of flux and g/t level. The data are tabulated in Table 9.

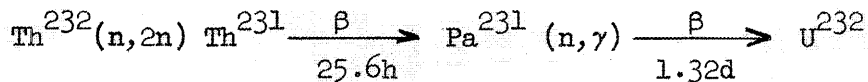
Figs. 27 and 28: Plots showing Ru^{103} and Ru^{106} activities as a function of decay time.

Fig. 29: Composite plot showing total ruthenium activity as a function of decay time.

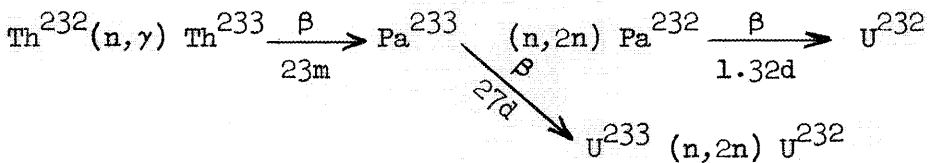
Figs. 30 and 31: Plots showing activities at time of discharge of Ba^{140} and La^{140} as a function of flux and g/t level and of decay time, respectively. The buildup data are tabulated in Table 10.

3.0 FORMATION OF U^{232} FROM Th^{232}

There are three paths by which U^{232} can be produced from Th^{232} , the predominant one being



There may be some production by either or both of the paths



but it is believed that these paths are less important. The ($n,2n$) cross sections of the appropriate isotopes for these two paths are unknown but probably are no higher than the ($n,2n$) cross section of Th^{232} .

In any of these cases an ($n,2n$) reaction is involved, and this reaction can occur only with neutrons with energy greater than the 5-6 Mev neutron

Table 6. Effect of U^{232} Concentration on Total α Activity of Product

Flux = 10^{14} n/cm²/sec; values at any other condition of flux and g/t level can be obtained by multiplying by the appropriate correction factor from Table 6a.

$\phi T \times 10^{-14}$ (n-days/cm ² /sec)	$U^{233} + Pa^{233}$ (moles per mole Th^{232})	U^{233} Disintegration (moles/yr·mole Th)	U^{232} at 5 mb Cross Section (moles/ 10^6 moles Th^{232})	U^{232} Disintegration (moles/yr·mole Th)	U^{232}/U^{233} α Activity Ratio, U^{232} Disintegration U^{233} Disintegration
17.11	9.957×10^{-4}	42.616×10^{-10}	2.636×10^{-2}	2.609×10^{-10}	6.122×10^{-2}
36.34	19.914×10^{-4}	85.232×10^{-10}	1.142×10^{-1}	1.130×10^{-9}	1.326×10^{-1}
58.65	29.871×10^{-4}	127.848×10^{-10}	2.850×10^{-1}	2.822×10^{-9}	2.207×10^{-1}
85.11	39.828×10^{-4}	170.464×10^{-10}	5.709×10^{-1}	5.652×10^{-9}	3.316×10^{-1}
117.2	49.785×10^{-4}	213.080×10^{-10}	1.022	1.012×10^{-8}	4.749×10^{-1}
207.6	69.699×10^{-4}	298.312×10^{-10}	2.776	2.748×10^{-8}	9.212×10^{-1}
503	99.570×10^{-4}	426.160×10^{-10}	11.316	1.120×10^{-7}	2.628

ORNL-LR-DWG 1661A

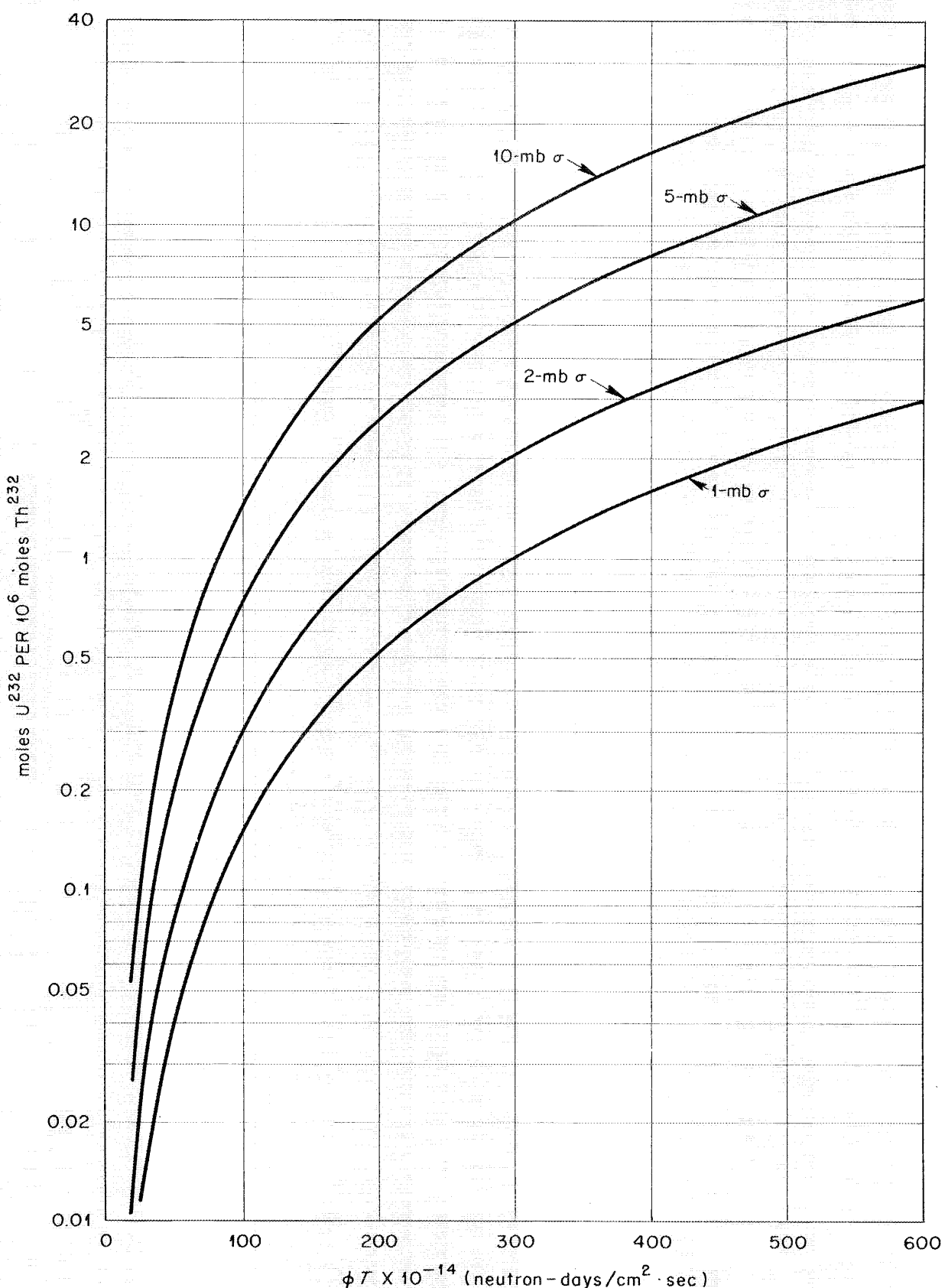


Fig. 13. Effect of Processing Period and Flux on U^{232} Concentration at Time of Discharge.

ORNL-LR-DWG 1662A

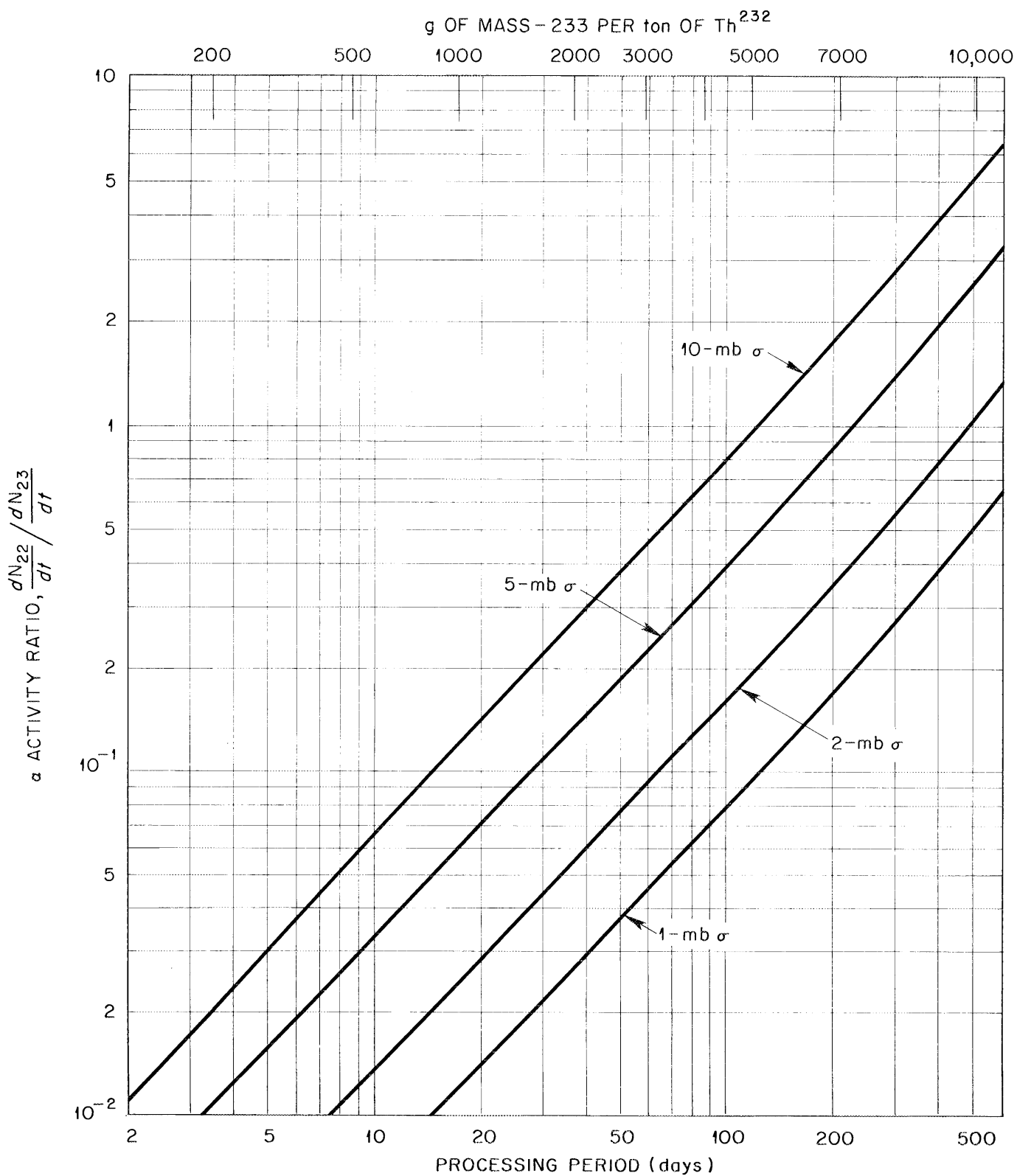


Fig. 14. Effect of Processing Period and $(n, 2n)$ Cross Section on U^{232}/U^{233} α Activity Ratio at Time of Discharge. Values Apply at Flux of 10^{14} neutrons/cm²·sec. Ratios at Other Flux Values are Multiplied by Correction Factor from Fig. 14a.

Table 6a. Correction Factors for U^{232}/U^{233} α Activity Ratios:
Based on Data Presented for 10^{14} Flux

g Mass 233 per ton Th ²³²	Correction Factor				
	10^{13}	5×10^{13}	10^{14}	5×10^{14}	10^{15}
1,000	1.0649	1.0193	1	0.9753	0.9708
2,000	1.1226	1.0692	1	0.9291	0.9142
3,000	1.1900	1.0691	1	0.8870	0.8470
4,000	1.2189	1.0930	1	0.8164	0.7774
5,000	1.2681	1.1164	1	0.7577	0.7052
7,000	1.3876	1.1718	1	0.6354	0.5594
10,000	1.7950	1.3260	1	0.4292	0.3362

Table 7. U^{232} Concentration and U^{232}/U^{233} α Activity Ratio at Various Fluxes as a function of g/t Level

g Mass ^{233}U per ton ^{232}Th	10^{13} Flux		5×10^{13} Flux		5×10^{14} Flux		10^{15} Flux	
	U^{232} 5 mb Cross Section (moles per 10^6 moles ^{232}Th)	α Activity Ratio, dN_{22}/dt / dN_{23}/dt	U^{232} 5 mb Cross Section (moles per 10^6 moles ^{232}Th)	α Activity Ratio, dN_{22}/dt / dN_{23}/dt	U^{232} 5 mb Cross Section (moles per 10^6 moles ^{232}Th)	α Activity Ratio, dN_{22}/dt / dN_{23}/dt	U^{232} 5 mb Cross Section (moles per 10^6 moles ^{232}Th)	α Activity Ratio, dN_{22}/dt / dN_{23}/dt
1,000	0.02807	0.0652	0.02687	0.0624	0.02571	0.0597	0.02559	0.0594
2,000	0.1282	0.1488	0.1221	0.1418	0.1061	0.1232	0.1044	0.1212
3,000	0.3338	0.2626	0.3047	0.2359	0.2488	0.1958	0.2414	0.1869
4,000	0.6959	0.4042	0.6240	0.3624	0.4661	0.2707	0.4438	0.2578
5,000	1.296	0.6022	1.141	0.5302	0.7744	0.3598	0.7207	0.3349
7,000	3.852	1.278	3.253	1.079	1.764	0.5853	1.553	0.5153
10,000	20.313	4.717	15.005	3.485	4.857	1.128	3.804	0.8835

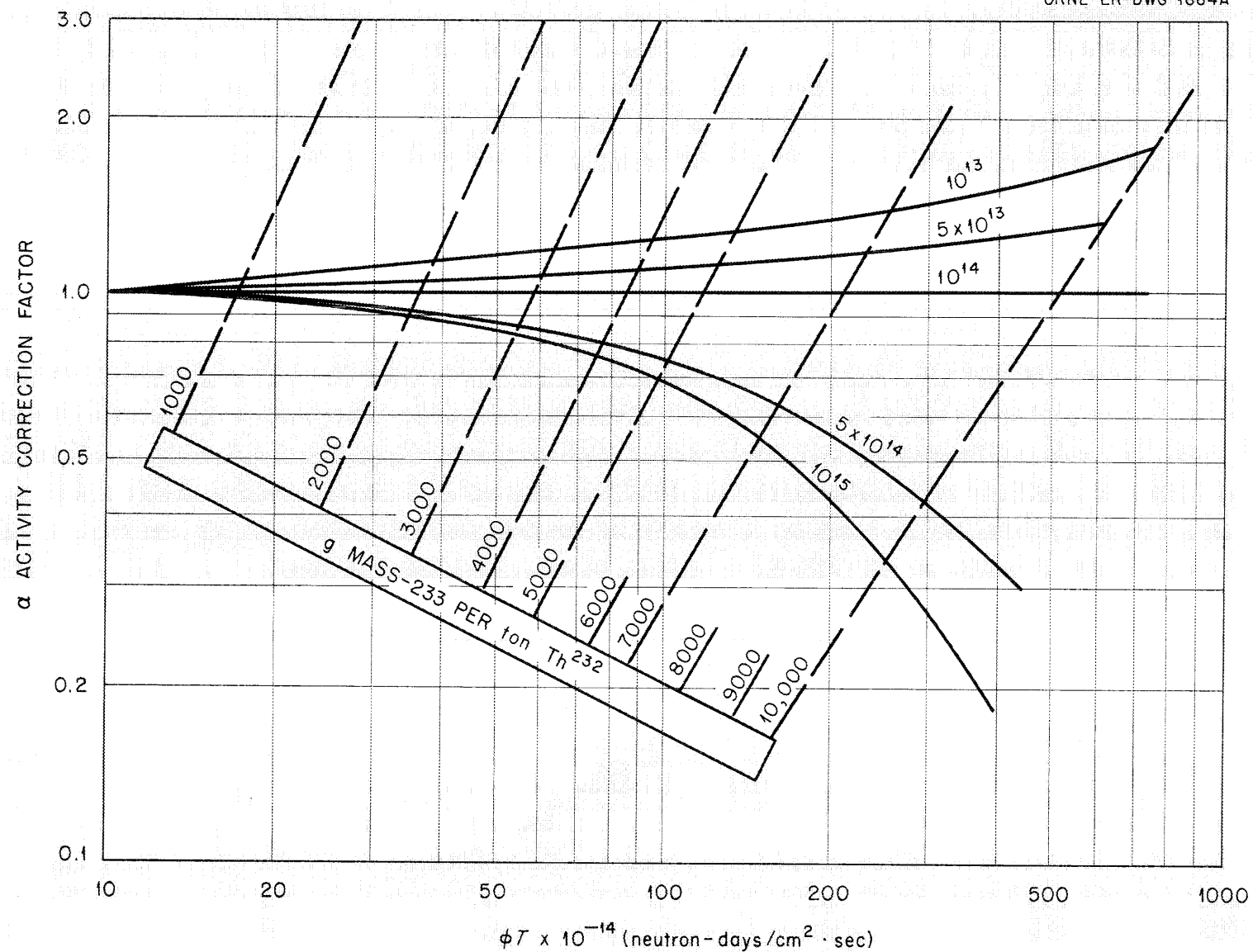


Fig. 14a. Correction Factor for U^{232} α Activity Ratio as a Function of Flux and g/t Level
(for use with Fig. 14.).

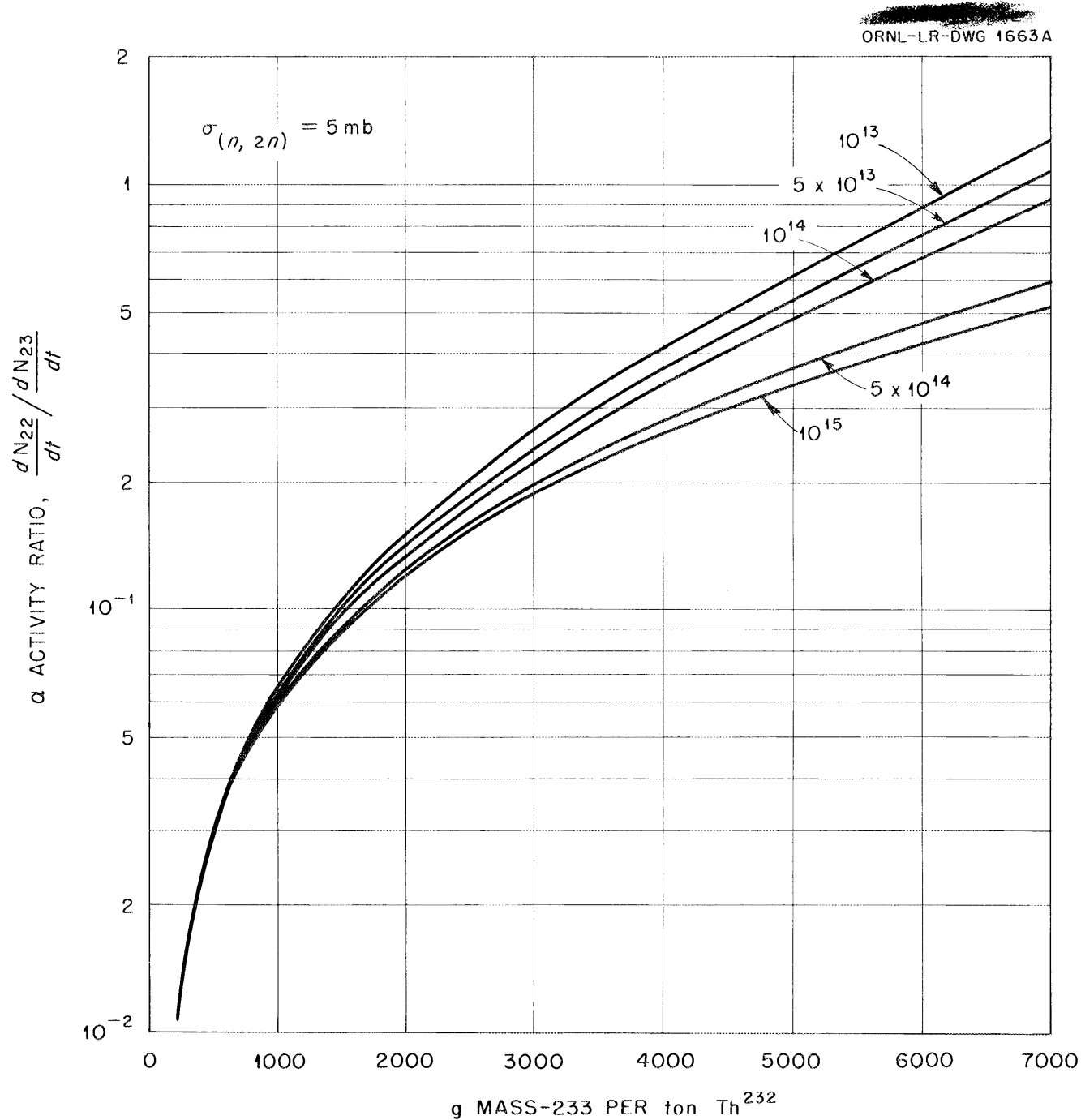


Fig. 15. Effect of Flux and g/t Level on U²³²/U²³³ α Activity Ratio at Time of Discharge.

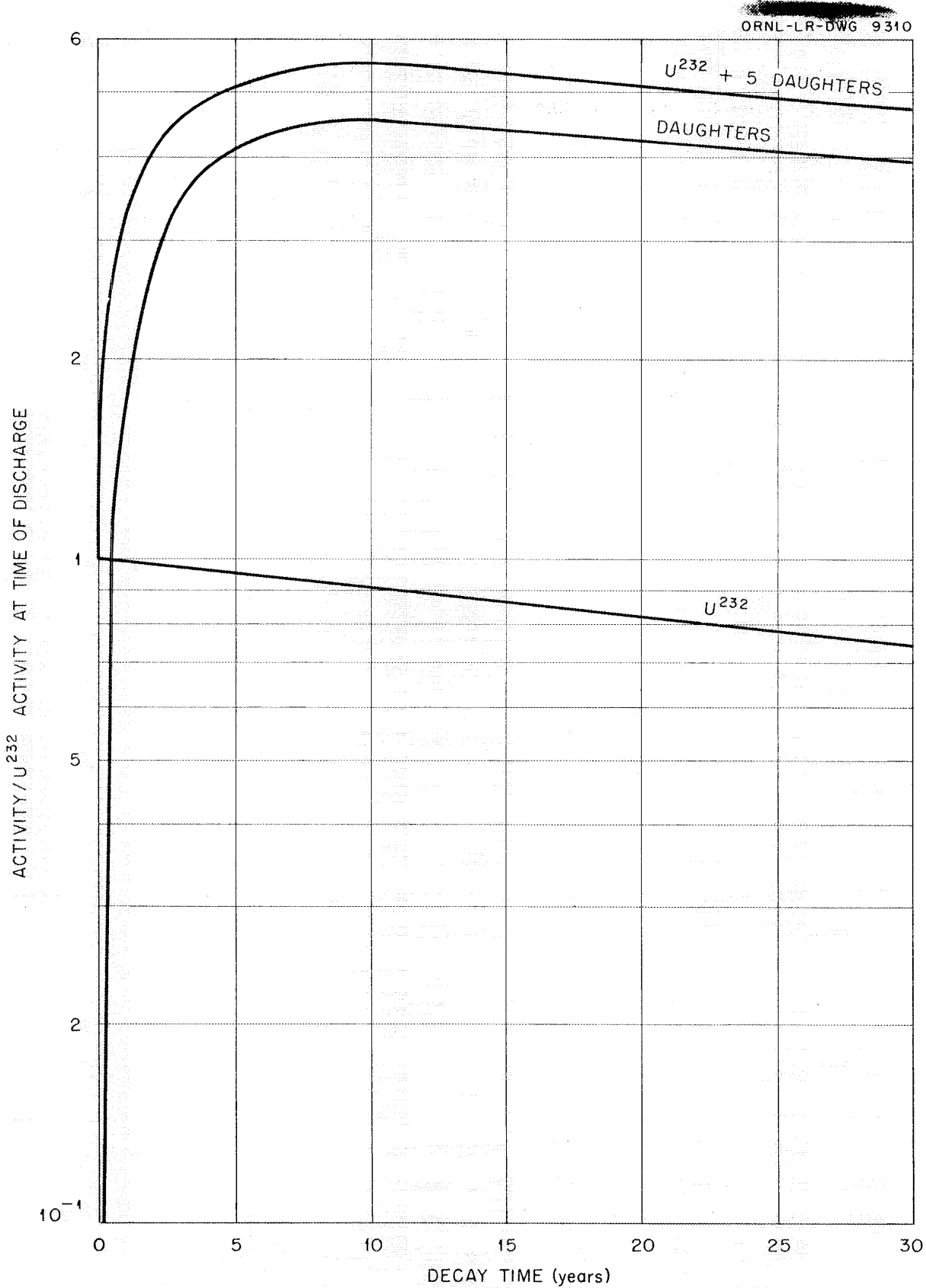


Fig. 16. Effect of Decay Time on U^{232} and Daughter Activities.

binding energy. Because of the high energy necessary for reaction, only a small fraction of neutrons enter into ($n,2n$) reactions, and this small fraction decreases with increased moderation of the reactor.

The ($n,2n$) cross sections for reactor neutrons have been variously reported as 2-13 mb, although there have been some data indicating ~ 1 mb. The differential equations used to calculate U^{232} concentration and activity are

$$\frac{dN_{22}}{dt} = N_{11} \phi \sigma_{11} - N_{22} C = 0$$

$$\frac{dN_{11}}{dt} = \phi N_{02} \sigma(n,2n)(Th) - N_{11} \phi \sigma_{11} - N_{11} C = 0$$

Then equations are integrated to give

$$N_{11} = \frac{\phi N_{02} \sigma(n,2n)(Th)}{\phi \sigma_{11} + C}$$

$$N_{22} = \frac{\phi N_{02} \sigma(n,2n)(Th) \phi \sigma_{11}}{C(\phi \sigma_{11} + C)}$$

$$\frac{N_{22}}{N_{02}} = \frac{\phi^2 \sigma(n,2n)(Th) \sigma_{11}}{C(\phi \sigma_{11} + C)}$$

In order to compare U^{233} products produced at different g/t levels or by decay of isolated Pa^{233} , it is necessary to determine the α activity due to U^{232} . This is done by determining the α activity ratio:

$$\alpha \text{ activity ratio} = \left(\frac{dN_{22}}{dt} \right) / \left(\frac{dN_{23}}{dt} \right) = \frac{N_{22} \lambda_{22}}{N_{23} \lambda_{23}}$$

U^{232} decays to a series of α -emitting daughters (Table 11) with a half-life of 1.9y, the half-life of Th^{228} . Hence in 1.9y the daughter activities are equal to half their equilibrium value. After 10 years the total α activity reaches a maximum of 5.2 times the U^{232} activity at time of reactor discharge, or 5.7 times the U^{232} activity then present.

With $N^0 = 0$ and neglecting the half-lives of the remainder of the series, the equation for the activity, A_s , of the daughter series as a

function of decay time after discharge becomes

$$A_s = 5A_{22}^o \frac{\lambda_{08}}{\lambda_{22} - \lambda_{08}} (e^{-\lambda_{22}t} - e^{-\lambda_{08}t})$$

Table 11. Daughters of U^{232}

Nuclide	Half-life	α (Mev)	% Decay by α Emission
U^{232}	70y	5.31	100
Th^{228}	1.9y	5.40	100
Ra^{224}	3.64d	5.68	100
Rn^{220}	55s	6.28	100
Po^{216}	0.16s	6.77	100
Pb^{212}	10.6h	--	0
$Bi^{212} (\alpha, \beta)$	60m	6.08	34
Po^{212a}	10^{-6} s	8.78	100

^a Only 66% of Pb^{212} formed in the chain reaches Po^{212} .

3.1 Comparison of U^{232} Content with that Produced during Batch Irradiation

The U^{233} product produced in continuous irradiations contains more U^{232} than that produced in batch irradiations, as reported in ORNL-1818. For comparison purposes the following activity values corresponding to a 2-mb ($n,2n$) cross section are used:

Table 12. α Activity Ratios at Various g/t Levels

g/t Level (Mass 233/ton Th)	Exponential Irradiation	Equilibrium Irradiation at Flux of 10^{14} n/cm ² /sec	Ratio
1,000	1.2×10^{-2}	2.4×10^{-2}	2
2,000	2.3×10^{-2}	5.6×10^{-2}	2.44
3,000	3.7×10^{-2}	9.0×10^{-2}	2.44
4,000	5×10^{-2}	1.35×10^{-1}	2.70
5,000	6.7×10^{-2}	1.9×10^{-1}	2.84
10,000	1.8×10^{-1}	1.05	5.82

Under equilibrium conditions the activities at the same g/t levels will be slightly higher for a lower flux or lower for a greater flux. However, even with the correction factor applied to a flux of 10^{15} n/cm²/sec, the U²³² activity will still be about a factor of 2 higher than that of exponential irradiations.

4.0 PRODUCTION AND DECAY OF Th²³⁴

Th²³⁴ activity will contribute to a radiation background in the thorium product from chemical processes. This activity will necessitate a long decay time since it is necessary to decay to 10^9 d/m/kg thorium for direct metallurgy. The activity of Th²³⁴ increases very markedly with increasing flux and increases asymptotically toward saturation activity as the g/t level increases. The Th²³⁴ saturation activity increases directly as the square of the flux. The minimum decay time to bring Th²³⁴ activity to 10^9 d/m/kg Th is 200d for all g/t levels at a flux of 10^{13} n/cm²/sec. If operation is at a flux of 5×10^{13} n/cm²/sec and Th²³⁴ saturates 310d decay would be required for this activity level to be reached.

5.0 EFFECT OF IRRADIATION PRODUCTS ON NEUTRON ECONOMY

Another consideration in the production of U²³³ is neutron economy. The intermediates in any chain may have high cross sections, and would remove neutrons which otherwise could be captured by thorium. The products considered in this study as poisons were Pa²³³, U²³⁴, and fission products. Other materials would contribute to neutron losses, but to a much lesser extent. The poison effect due to Pa²³³ increases markedly with flux and g/t level, while that due to U²³⁴ shows only a slight increase with flux and g/t level. On the other hand, the poison effects created by fission products are much higher at lower fluxes. This phenomenon is due mainly to the longer processing periods required at lower fluxes for a given g/t level. The overall poison effects show an increase with flux. The total poison at 5000 g/t changes from 2.237% at 10^{13} n/cm²/sec to 9.832% at 10^{15} n/cm²/sec flux. The poison effects were based on neutron losses to the given chain member as compared to neutrons captured by thorium²³².

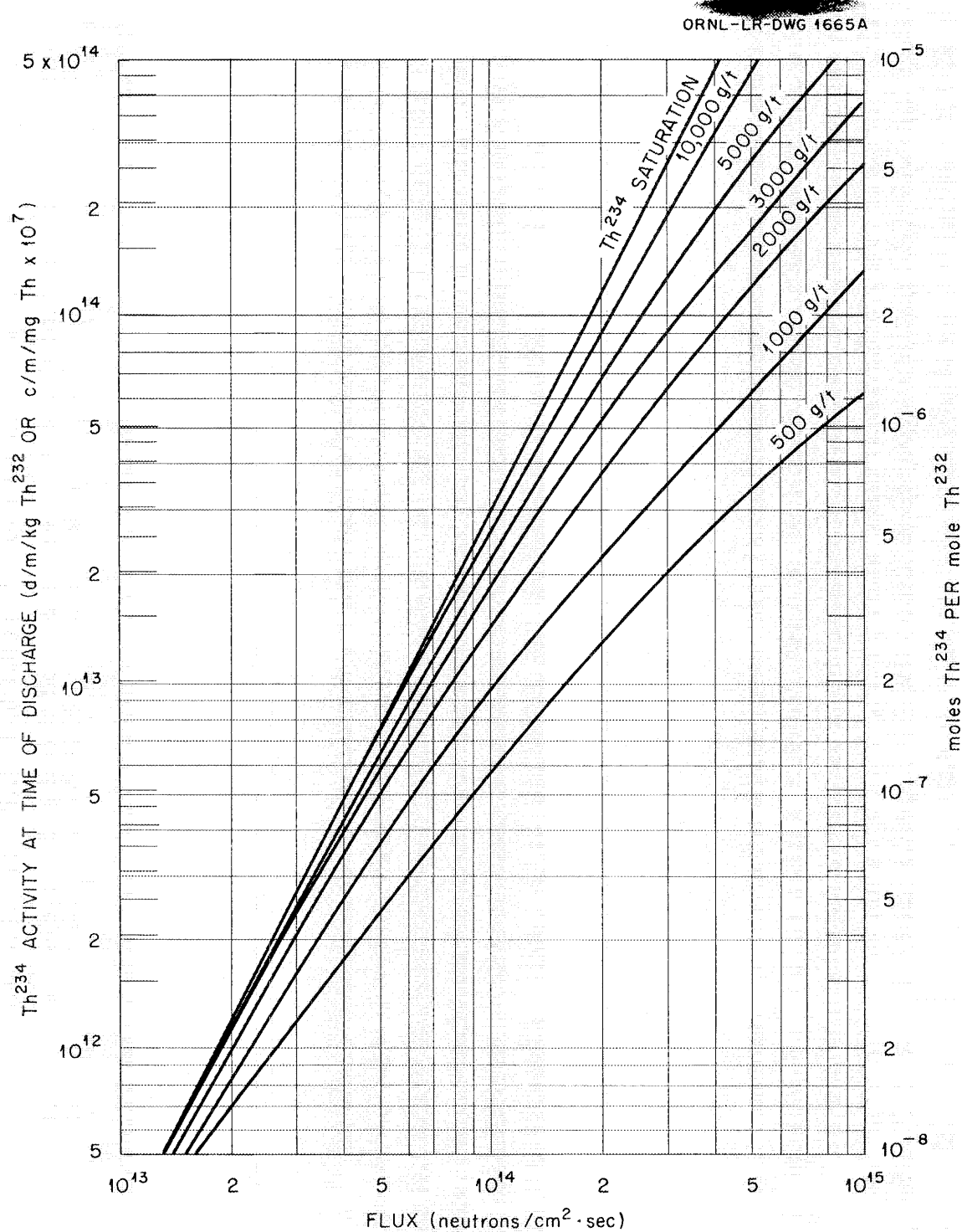


Fig. 17. Effect of Flux on Th²³⁴ Concentration and Activity at Time of Discharge. Th²³⁴ Saturation Value at Flux of 10¹⁵ neutrons/cm²·sec is 5.78×10^{-5} mole per mole of Th²³² or 2.99×10^{15} d/m/kg Th; at Flux of 10¹³ neutrons/cm²·sec Th²³⁴ Saturation Value is 5.78×10^{-9} mole per mole of Th²³² or 2.99×10^{11} d/m/kg Th.

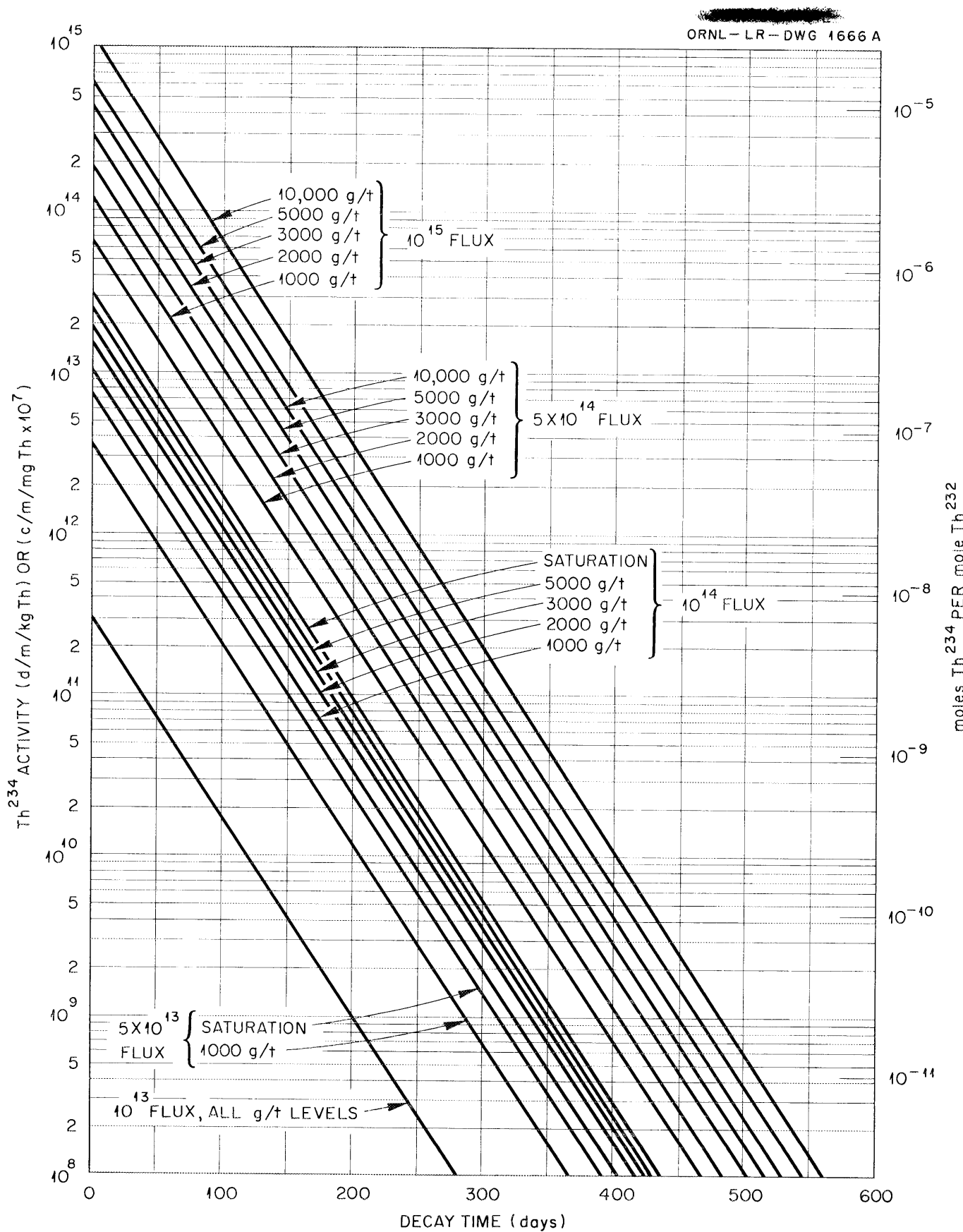


Fig.18. Effect of Decay Time on Th²³⁴ Concentration and Activity.

Table 8. Neutron Losses to Pa^{233} , U^{234} , and Fission Products

g Mass 233 per ton Th ²³²	$\frac{\phi_{N_{13}}}{\phi_{N_{02}}} \sigma_{13}$	$\frac{\phi_{N_{24}}}{\phi_{N_{02}}} \sigma_{24}$	$\frac{\phi_{N_{FP}}}{\phi_{N_{02}}} \sigma_{FP}$	Σ Losses
	$\times 10^2$ (To Pa ²³³)	$\times 10^2$ (To U ²³⁴)	$\times 10^2$ (To FP's)	$\phi_{N_{02}} \sigma_{02} \times 10^2$ (Total)
At Flux of 10^{13} n/cm ² /sec				
1,000	0.417	0.0111	0.0318	0.4599
2,000	0.462	0.0424	0.1537	0.6581
3,000	0.480	0.0985	0.3956	0.9741
4,000	0.489	0.1865	0.7985	1.4740
5,000	0.495	0.3163	1.4254	2.2367
7,000	0.502	0.7678	3.8177	5.0875
10,000	0.507	2.5588	16.5242	19.5900
At Flux of 5×10^{13} n/cm ² /sec				
1,000	1.1807	0.0158	0.0172	1.2137
2,000	1.6516	0.0581	0.1031	1.8128
3,000	1.8960	0.1258	0.2867	2.3085
4,000	2.0541	0.2271	0.6061	2.8873
5,000	2.1628	0.3700	1.1097	3.6425
7,000	2.3027	0.8407	3.0175	6.1609
10,000	2.4210	2.5234	12.0955	17.0399

ORNL-LR-DWG 1667A

NEUTRON CAPTURES IN HIGH CROSS-SECTION MATERIAL

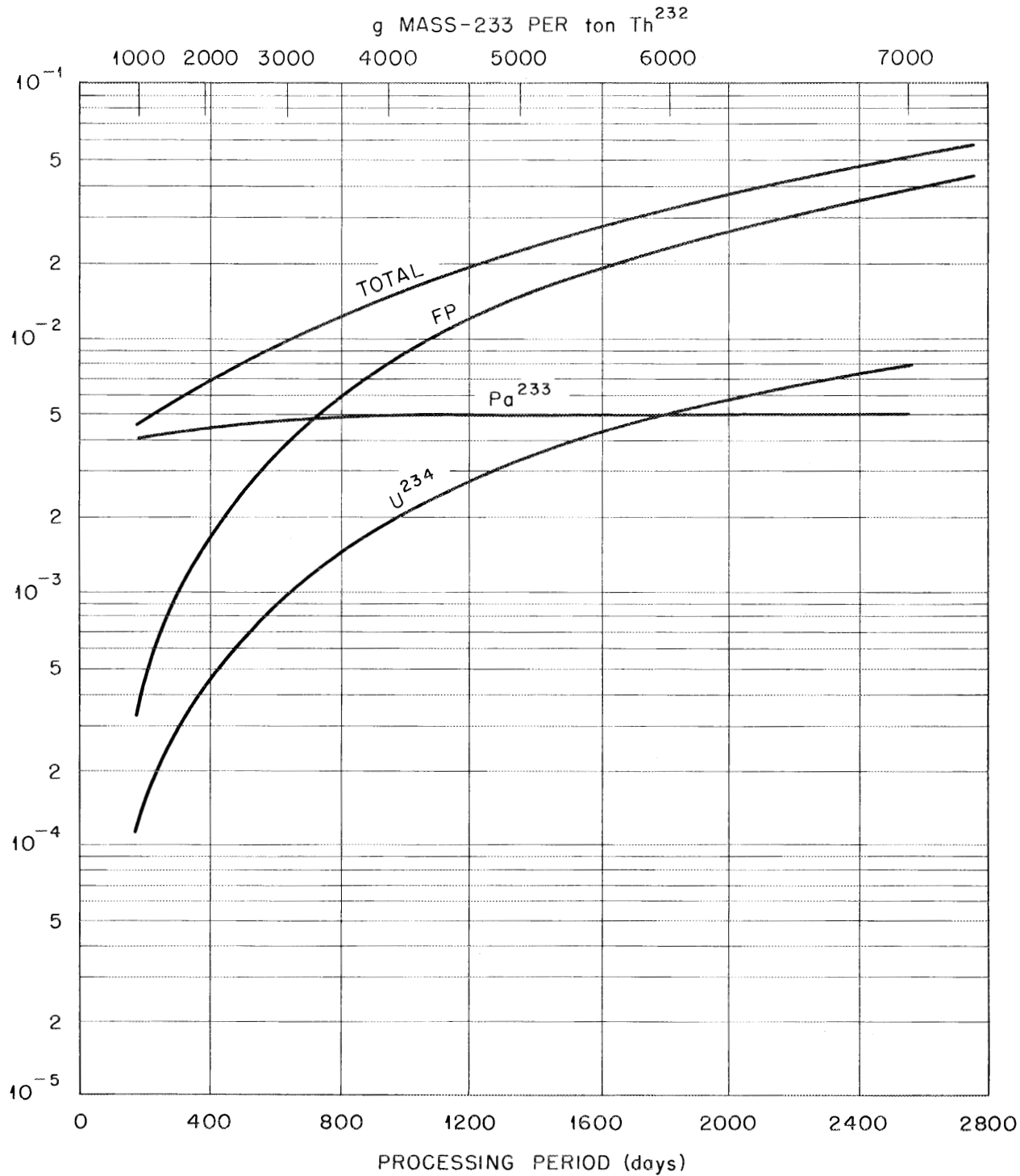


Fig. 19. Extraneous Neutron Captures at Flux of 10¹³ neutrons /cm² · sec

ORNL-LR-DWG 1668 A

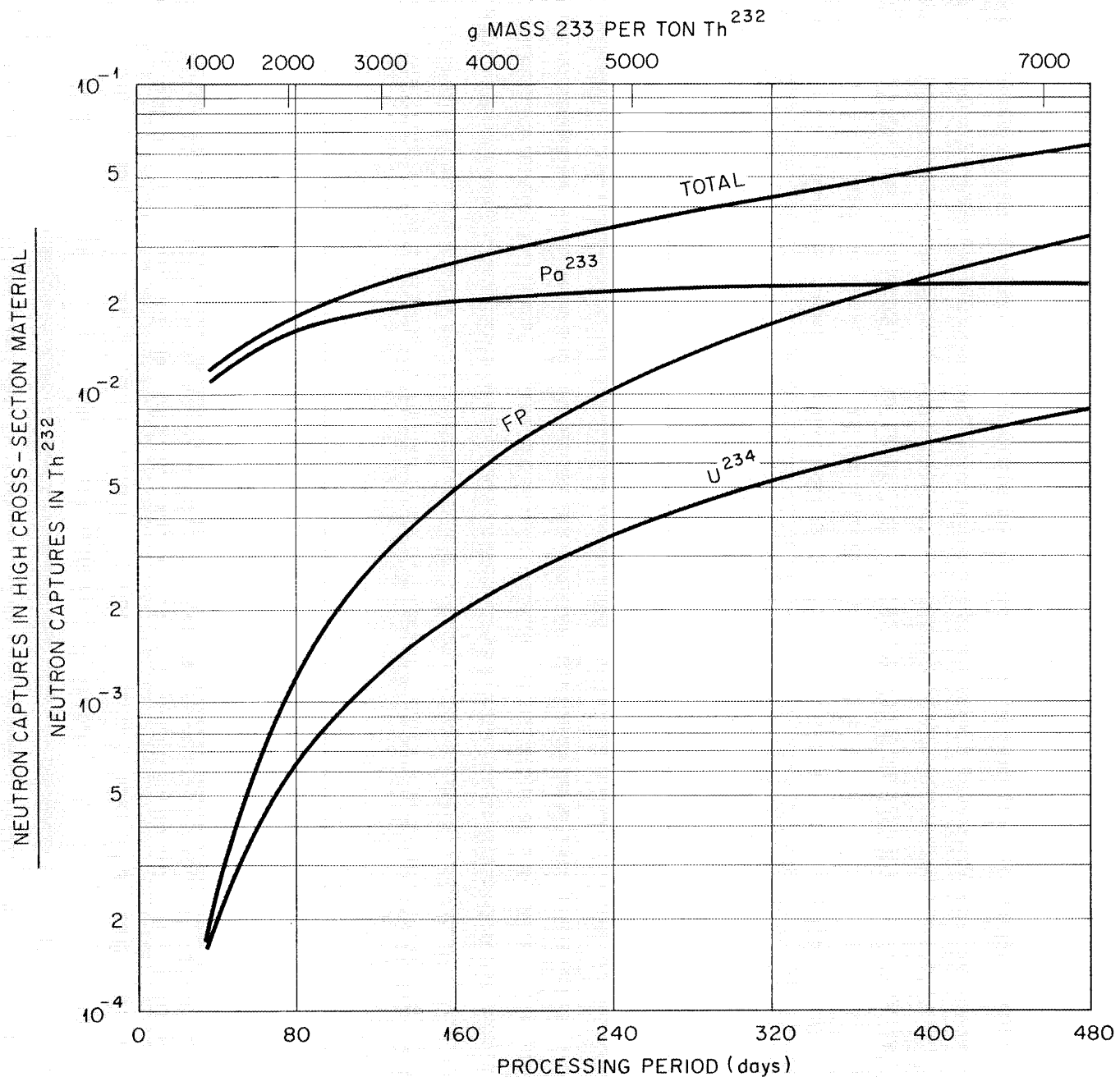


Fig. 20. Extraneous Neutron Captures at Flux of 5×10^{13} neutrons/cm²·sec.

Table 8 (continued)

g Mass 233 per ton Th ²³²	$\frac{\phi_{N_{13}}}{\phi_{N_{02}}} \sigma_{13}$	$\frac{\phi_{N_{24}}}{\phi_{N_{02}}} \sigma_{24}$	$\frac{\phi_{N_{FP}}}{\phi_{N_{02}}} \sigma_{FP}$	$\frac{\sum}{\phi_{N_{02}}} \sigma_{Losses}$
	σ_{02}	σ_{02}	σ_{02}	σ_{02}
	$\times 10^2$ (To Pa ²³³)	$\times 10^2$ (To U ²³⁴)	$\times 10^2$ (To FP's)	$\times 10^2$ (Total)
At Flux of 10^{14} n/cm ² /sec				
1,000	1.5242	0.0192	0.0073	1.5507
2,000	2.3948	0.0663	0.0712	2.5323
3,000	2.9693	0.1448	0.2107	3.3248
4,000	3.3797	0.2580	0.4594	4.0971
5,000	3.6891	0.4134	0.8563	4.9588
7,000	4.1256	0.9022	2.3497	7.3775
10,000	4.5340	2.4945	8.8505	15.8790
At Flux of 5×10^{14} n/cm ² /sec				
1,000	1.9774	0.0206	0.0027	2.0007
2,000	3.7075	0.0810	0.0205	3.8090
3,000	5.2530	0.1814	0.0657	5.5001
4,000	6.6578	0.3239	0.1499	7.1216
5,000	7.9480	0.5126	0.2863	8.7469
7,000	10.2630	1.0533	0.7801	12.0964
10,000	13.2379	2.4269	2.4696	18.1344
At Flux of 10^{15} n/cm ² /sec				
1,000	2.0526	0.0210	0.0014	2.0750
2,000	3.9685	0.0838	0.0108	4.0631
3,000	5.7765	0.1890	0.0351	6.0006
4,000	7.4974	0.3387	0.0807	7.9168
5,000	9.1423	0.5356	0.1544	9.8323
7,000	12.2588	1.0893	0.4155	13.7636
10,000	16.5835	2.4127	1.2477	20.2439

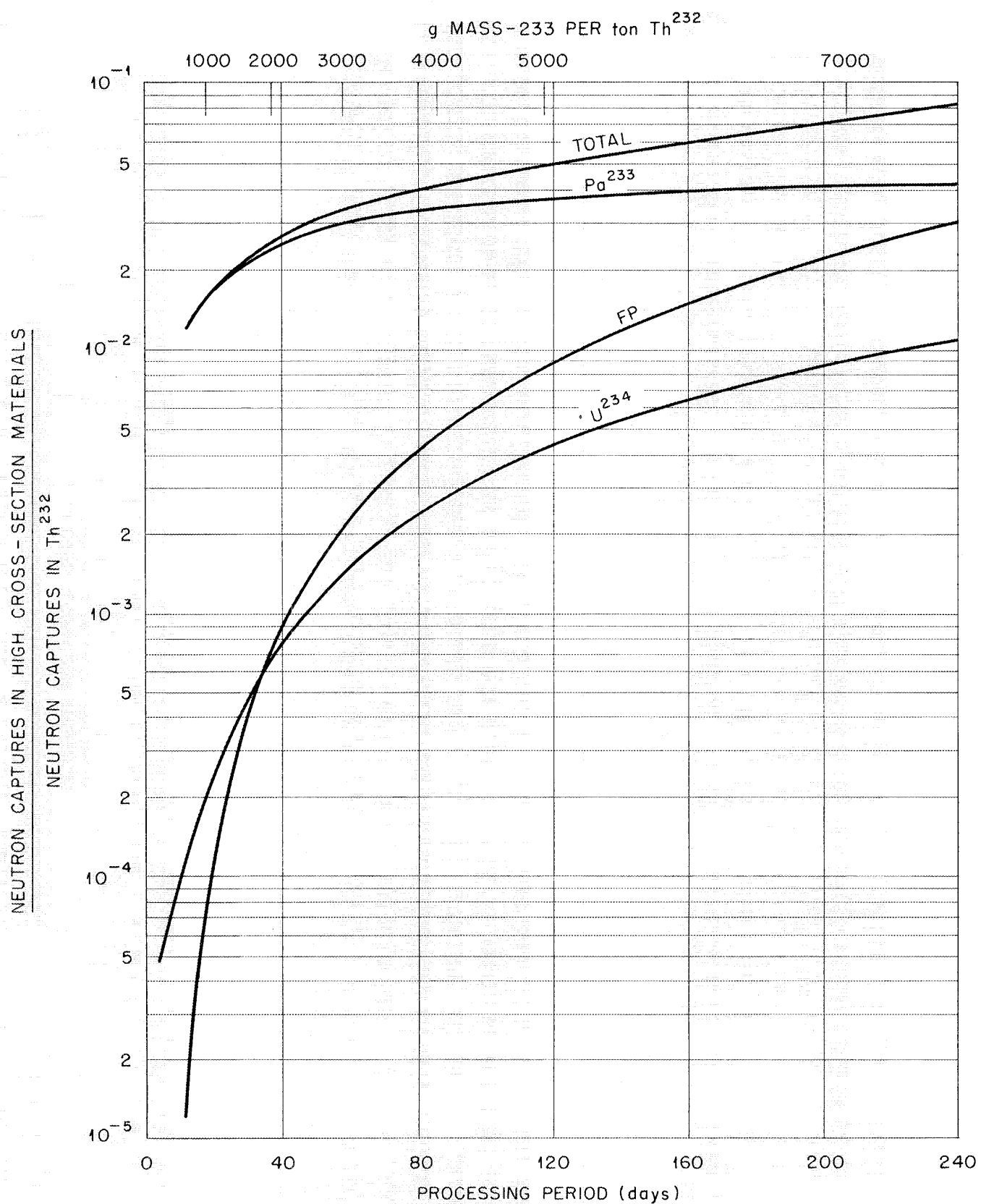


Fig. 21. Extraneous Neutron Captures at Flux of 10^{14} neutrons/cm² · sec.

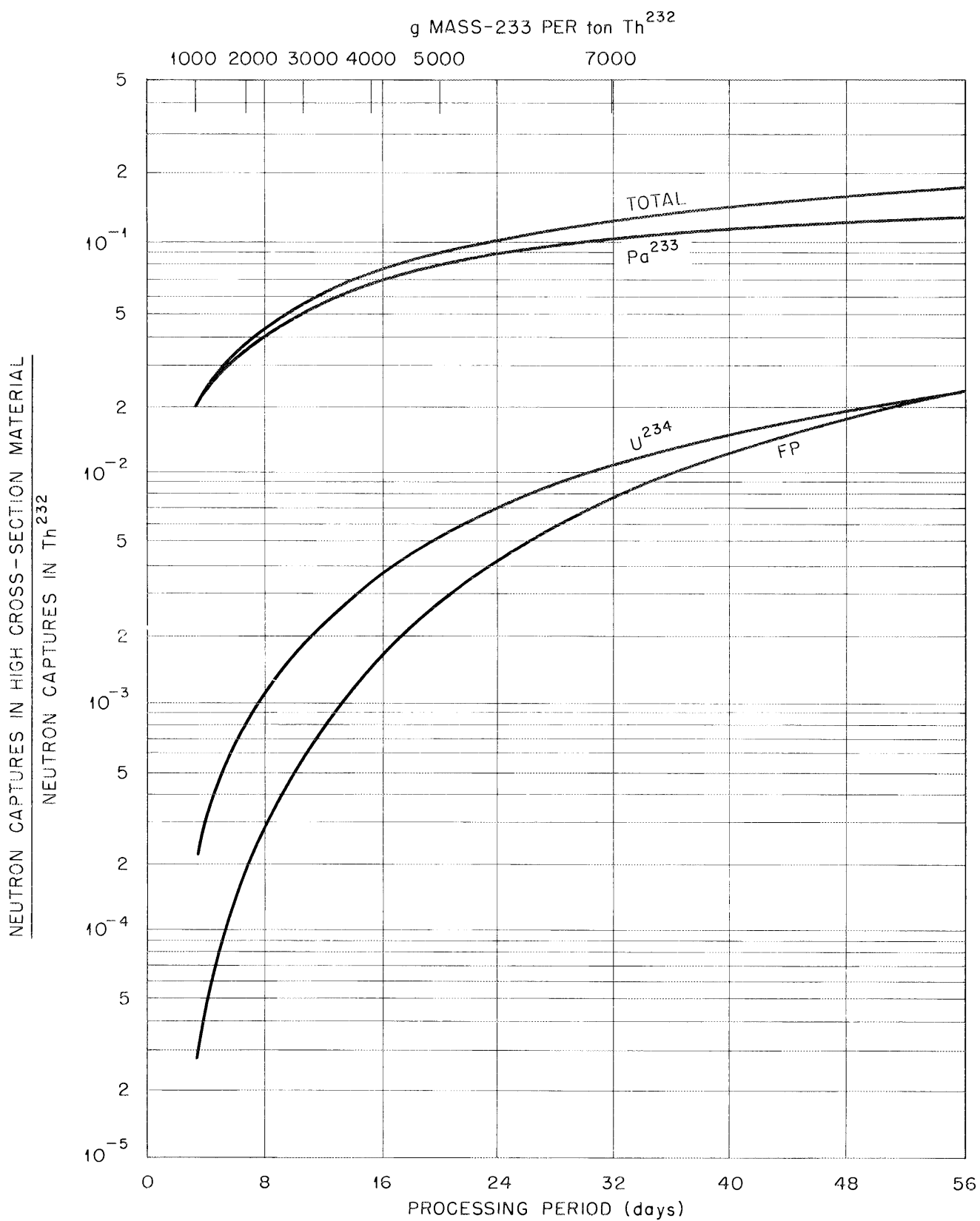


Fig. 22. Extraneous Neutron Captures at Flux of 5×10^{14} neutrons/cm² · sec.

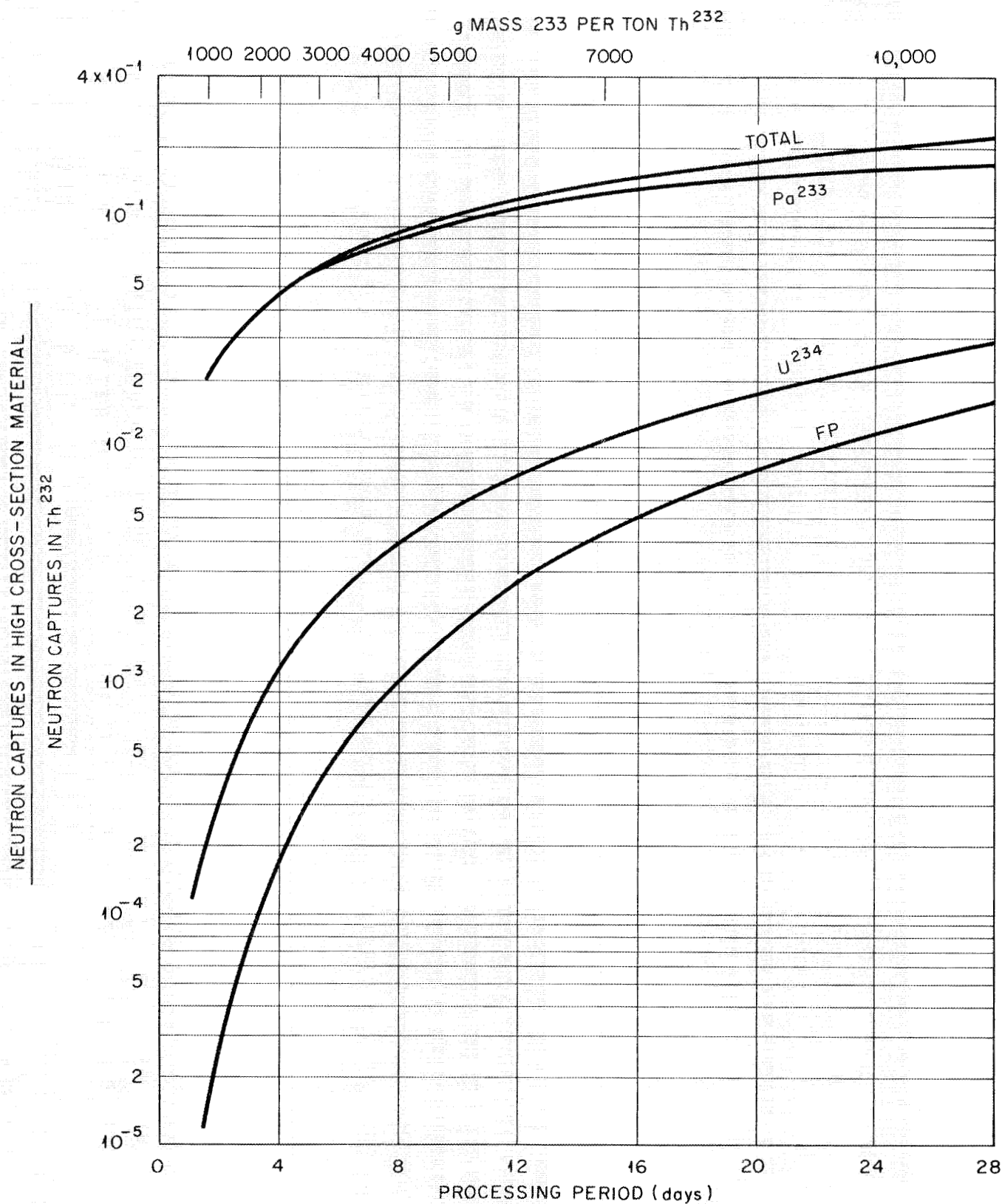


Fig. 23. Extraneous Neutron Captures at Flux of 10^{15} neutrons/cm²·sec.

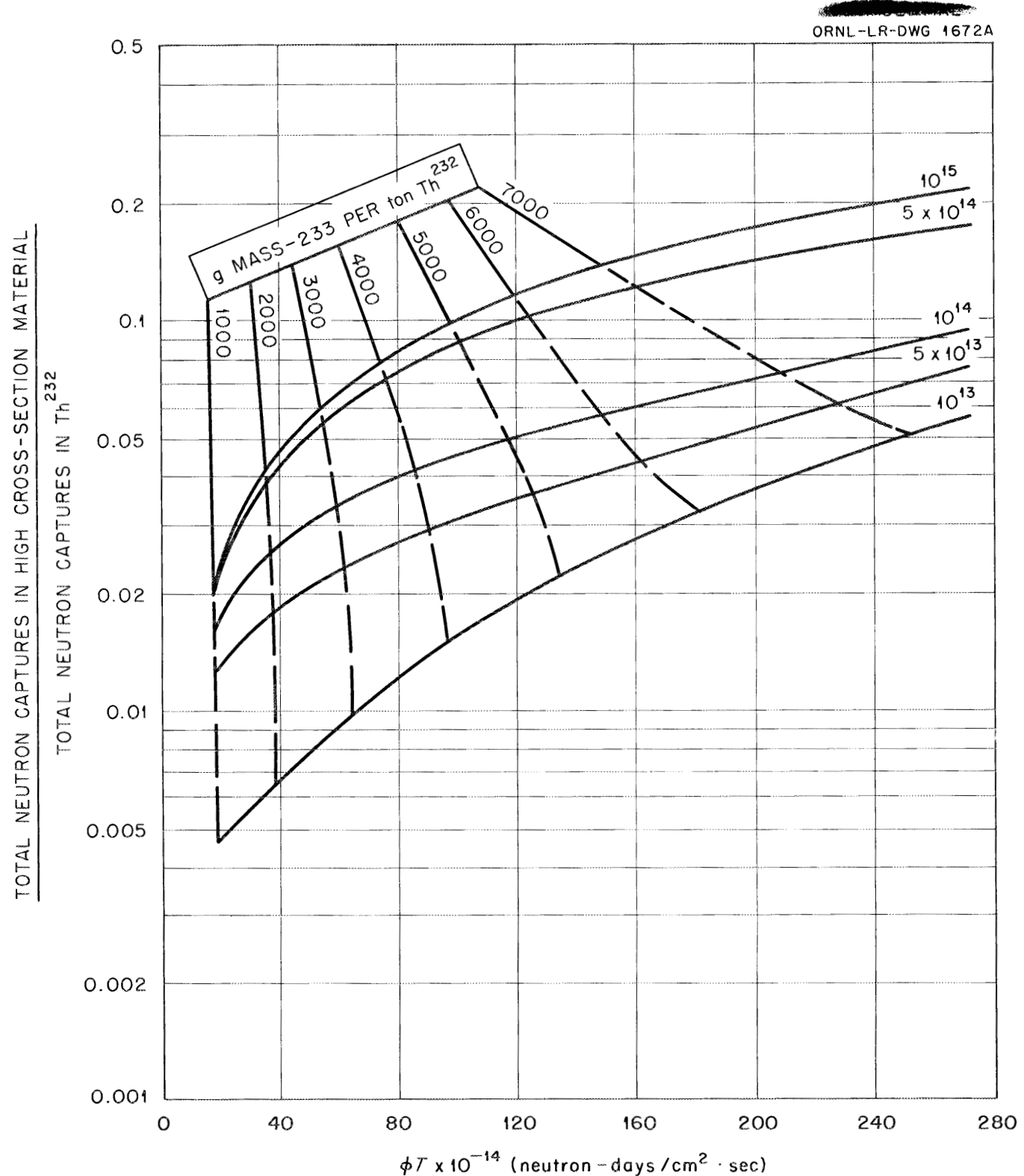


Fig. 24. Effect of Flux and Extent of Irradiation on Extraneous Neutron Captures.

The average cross section used for the fission products was 18b. This value was obtained by averaging the important high cross-section fission products. This indicated that nineteen fission products with a total yield of 47% contributed the major fraction of the fission product poison. If this poison contribution is averaged over 200% total yield an effective cross section of 17 - 21b can be assigned to the entire group.

6.0 IMPORTANCE OF RUTHENIUM AND THE Ba¹⁴⁰-La¹⁴⁰ CHAIN

The important fission products from the standpoint of thorium irradiation are Ru¹⁰³, Ru¹⁰⁶, and the Ba¹⁴⁰-La¹⁴⁰ chain. Ruthenium is difficult to separate in chemical processing cycles, and the high-energy gammas associated with La¹⁴⁰ determine shield design.

The ruthenium activity encountered in continuous irradiations are much higher than those encountered in batch irradiations. At a flux of 10^{13} n/cm²/sec and a 3000 g/t level, the Ru¹⁰³ and Ru¹⁰⁶ activities are almost twice those in batch irradiation. At fluxes of 10^{14} and 10^{15} n/cm²/sec the ratio is almost 3/1. For any given g/t level, there is a flux at which the ruthenium activity is a maximum (see Figs. 25 and 26). The flux value at which ruthenium activity is a maximum increases with the g/t level. The results of this study indicate that the chemical processing of the homogeneous blanket must provide good ruthenium decontamination if low-activity thorium is needed for fresh slurry production.

The lanthanum activity was presented to indicate the problems that may be encountered in shield design pertinent to the processing of high-level material. For production of 5000 g/t material under continuous irradiation at 5×10^{13} n/cm²/sec (approximately the flux of the TBR reactor), there will be 380 curies of La¹⁴⁰ per kilogram of thorium at discharge. Previous study of batch irradiations indicated that La¹⁴⁰ activity would be 10 curies/kg Th at 1000 g/t and a flux of 10^{13} n/cm²/sec. For any given g/t level there is a flux at which the lanthanum activity is a maximum. The flux value at which lanthanum activity is a maximum also increases with the g/t level.

Table 9. Ruthenium Isotope Concentrations and Activities at Time of Discharge

g Mass 233 per ton Th ²³²	Processing Rate (reactor vol/day)	Ru ¹⁰³		Ru ¹⁰⁶	
		Conc. (atoms/mole Th)	Activity (d/m/kg Th)	Conc. (atoms/mole Th)	Activity (d/m/kg Th)
At Flux of 10^{13} n/cm ² /sec					
1,000	5.66×10^{-3}	8.512×10^{16}	4.402×10^{12}	6.145×10^{16}	4.396×10^{11}
2,000	2.59×10^{-3}	2.177×10^{17}	1.126×10^{13}	2.200×10^{17}	1.574×10^{12}
3,000	1.57×10^{-3}	3.571×10^{17}	1.847×10^{13}	4.31×10^{17}	3.08×10^{12}
4,000	1.05×10^{-3}	4.989×10^{17}	2.580×10^{13}	6.72×10^{17}	4.80×10^{12}
5,000	7.5×10^{-4}	6.410×10^{17}	3.316×10^{13}	9.40×10^{17}	6.72×10^{12}
7,000	3.9×10^{-4}	9.283×10^{17}	4.800×10^{13}	1.493×10^{18}	1.068×10^{13}
10,000	1.3×10^{-4}	1.360×10^{18}	7.034×10^{13}	2.38×10^{18}	1.70×10^{13}
At Flux of 5×10^{13} n/cm ² /sec					
1,000	2.893×10^{-2}	1.174×10^{17}	6.072×10^{12}	4.382×10^{16}	3.134×10^{11}
2,000	1.329×10^{-2}	4.869×10^{17}	2.518×10^{13}	2.403×10^{17}	1.719×10^{12}
3,000	8.23×10^{-3}	1.004×10^{18}	5.192×10^{13}	6.111×10^{17}	4.372×10^{12}
4,000	5.60×10^{-3}	1.611×10^{18}	8.332×10^{13}	1.168×10^{18}	8.356×10^{12}
5,000	4.01×10^{-3}	2.272×10^{18}	1.175×10^{14}	1.913×10^{18}	1.368×10^{13}
7,000	2.19×10^{-3}	3.688×10^{18}	1.907×10^{14}	3.972×10^{18}	2.842×10^{13}
10,000	8.2×10^{-4}	5.939×10^{18}	3.071×10^{14}	8.493×10^{18}	6.076×10^{13}

Table 9 (continued)

g Mass 233 per ton Th ²³²	Processing Rate (reactor vol/day)	^{Ru} ¹⁰³		^{Ru} ¹⁰⁶	
		Conc. (atoms/mole Th)	Activity (d/m/kg Th)	Conc. (atoms/mole Th)	Activity (d/m/kg Th)
At Flux of 10^{14} n/cm ² /sec					
1,000	5.843×10^{-2}	9.170×10^{16}	4.742×10^{12}	2.886×10^{16}	2.065×10^{11}
2,000	2.752×10^{-2}	4.758×10^{17}	2.461×10^{13}	1.803×10^{17}	1.290×10^{12}
3,000	1.705×10^{-2}	1.138×10^{18}	5.886×10^{13}	5.085×10^{17}	3.639×10^{12}
4,000	1.175×10^{-2}	2.021×10^{18}	1.045×10^{14}	1.050×10^{18}	7.511×10^{12}
5,000	8.53×10^{-3}	3.077×10^{18}	1.591×10^{14}	1.840×10^{18}	1.316×10^{13}
7,000	4.82×10^{-3}	5.562×10^{18}	2.876×10^{14}	4.321×10^{18}	3.091×10^{13}
10,000	1.99×10^{-3}	9.912×10^{18}	5.126×10^{14}	1.106×10^{19}	7.913×10^{13}
At Flux of 5×10^{14} n/cm ² /sec					
1,000	29.59×10^{-2}	2.843×10^{16}	1.470×10^{12}	7.539×10^{15}	5.394×10^{10}
2,000	14.30×10^{-2}	1.990×10^{17}	1.029×10^{13}	5.545×10^{16}	3.967×10^{11}
3,000	9.158×10^{-2}	6.008×10^{17}	3.107×10^{13}	1.759×10^{17}	1.258×10^{12}
4,000	6.555×10^{-2}	1.290×10^{18}	6.672×10^{13}	3.978×10^{17}	2.847×10^{12}
5,000	4.975×10^{-2}	2.310×10^{18}	1.195×10^{14}	7.514×10^{17}	5.375×10^{12}
7,000	3.136×10^{-2}	5.469×10^{18}	2.828×10^{14}	1.994×10^{18}	1.427×10^{13}
10,000	1.717×10^{-2}	1.338×10^{19}	6.920×10^{14}	5.963×10^{18}	4.266×10^{13}
At Flux of 10^{15} n/cm ² /sec					
1,000	59.31×10^{-2}	1.513×10^{16}	7.825×10^{11}	3.918×10^{15}	2.802×10^{10}
2,000	28.83×10^{-2}	1.114×10^{17}	5.761×10^{12}	2.960×10^{16}	2.118×10^{11}
3,000	18.61×10^{-2}	3.499×10^{17}	1.810×10^{13}	9.542×10^{16}	6.828×10^{11}
4,000	13.46×10^{-2}	7.780×10^{17}	4.024×10^{13}	2.181×10^{17}	1.560×10^{12}
5,000	10.35×10^{-2}	1.439×10^{18}	7.442×10^{13}	4.151×10^{17}	2.970×10^{12}
7,000	6.746×10^{-2}	3.598×10^{18}	1.861×10^{14}	1.104×10^{18}	7.898×10^{12}
10,000	3.989×10^{-2}	9.469×10^{18}	4.897×10^{14}	3.238×10^{18}	2.317×10^{13}

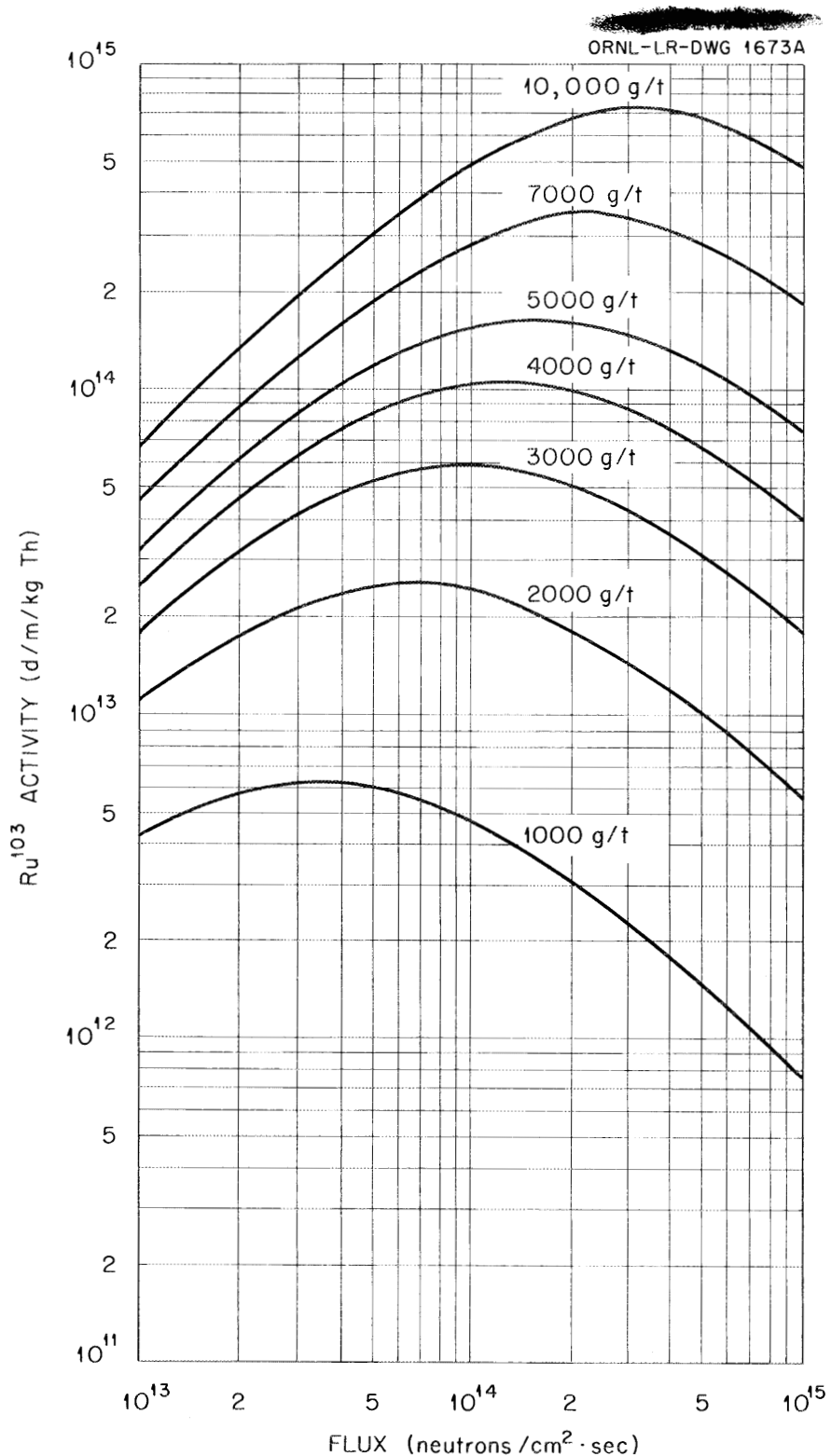


Fig. 25. Effect of Flux and g/t Level on Ru^{103} Activity at Time of Discharge.

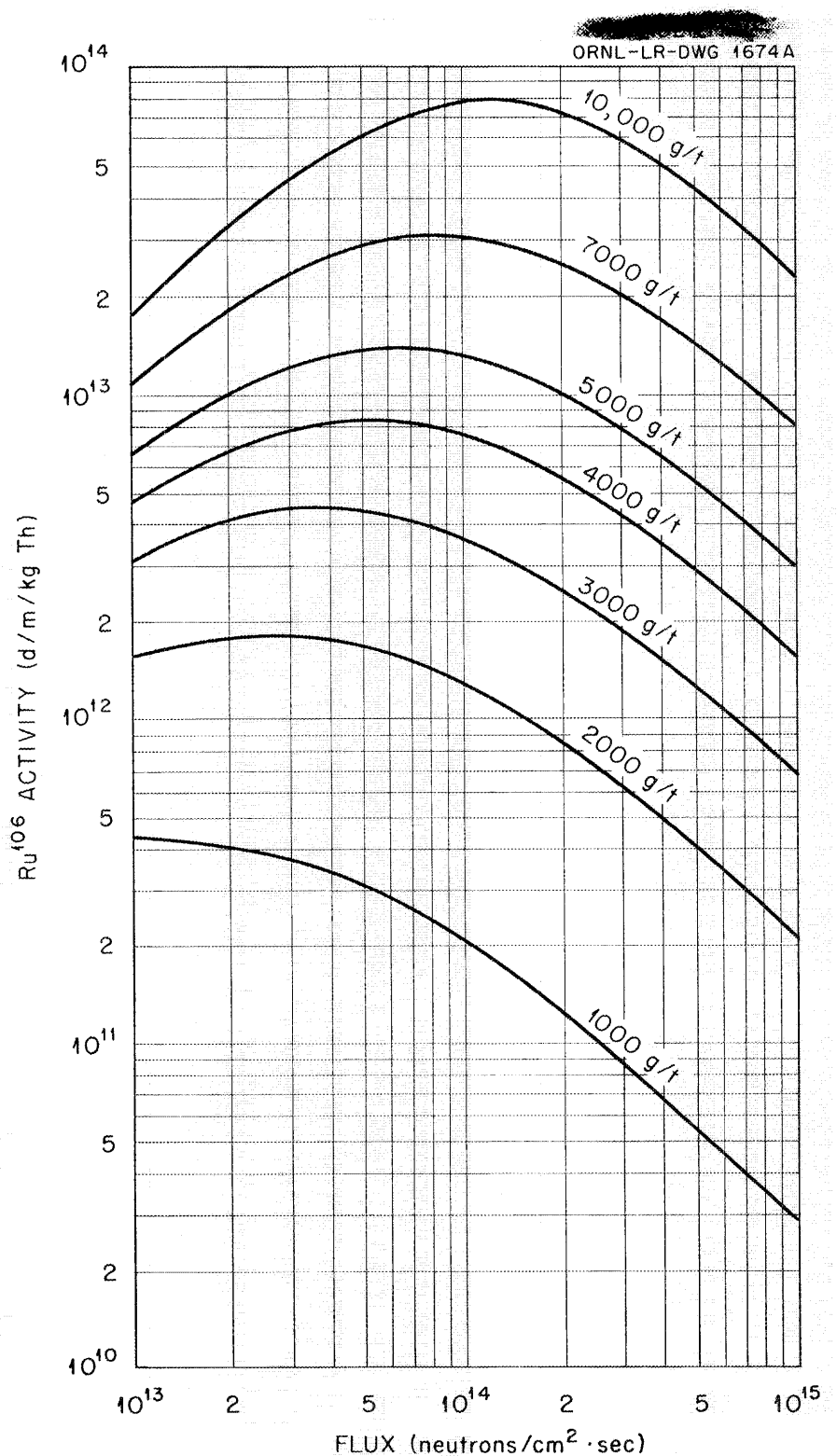


Fig. 26. Effect of Flux and g/t Level on Ru¹⁰⁶ Activity at Time of Discharge.

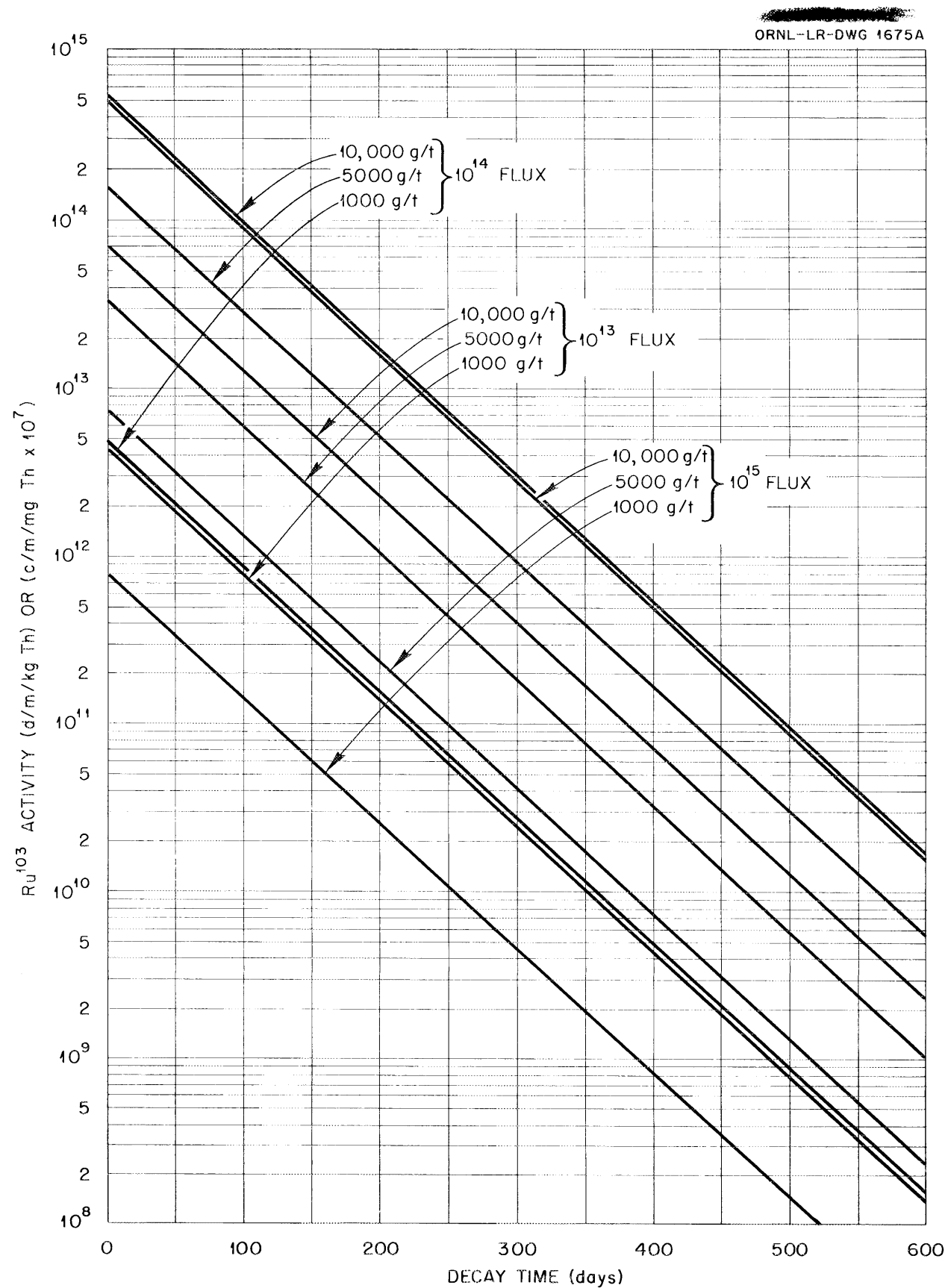


Fig. 27. Effect of Decay Time on Ru^{103} Activity.

ORNL-LR-DWG 1676A

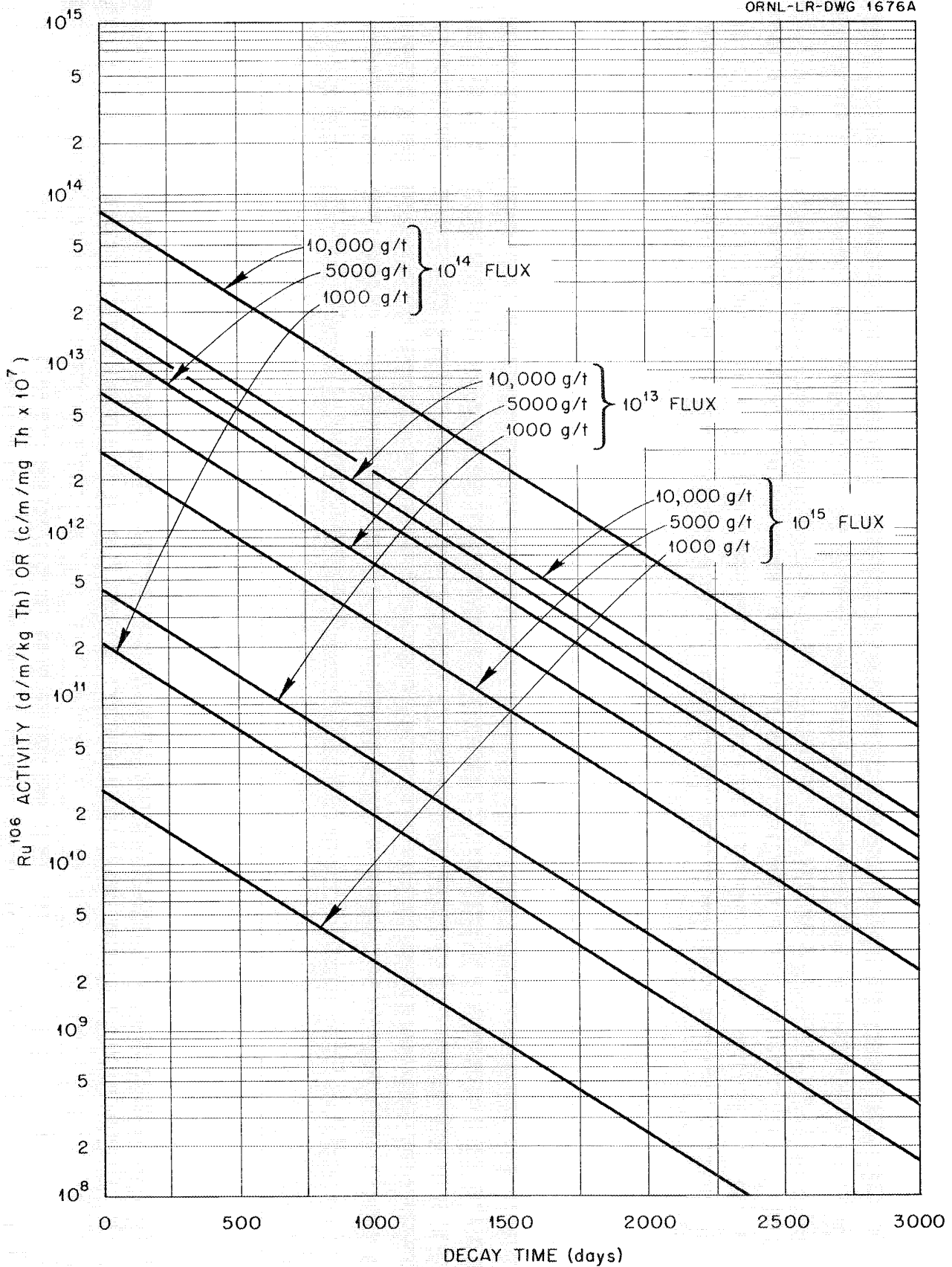


Fig. 28. Effect of Decay Time on Ru^{106} Activity.

ORNL-LR-DWG 1677A

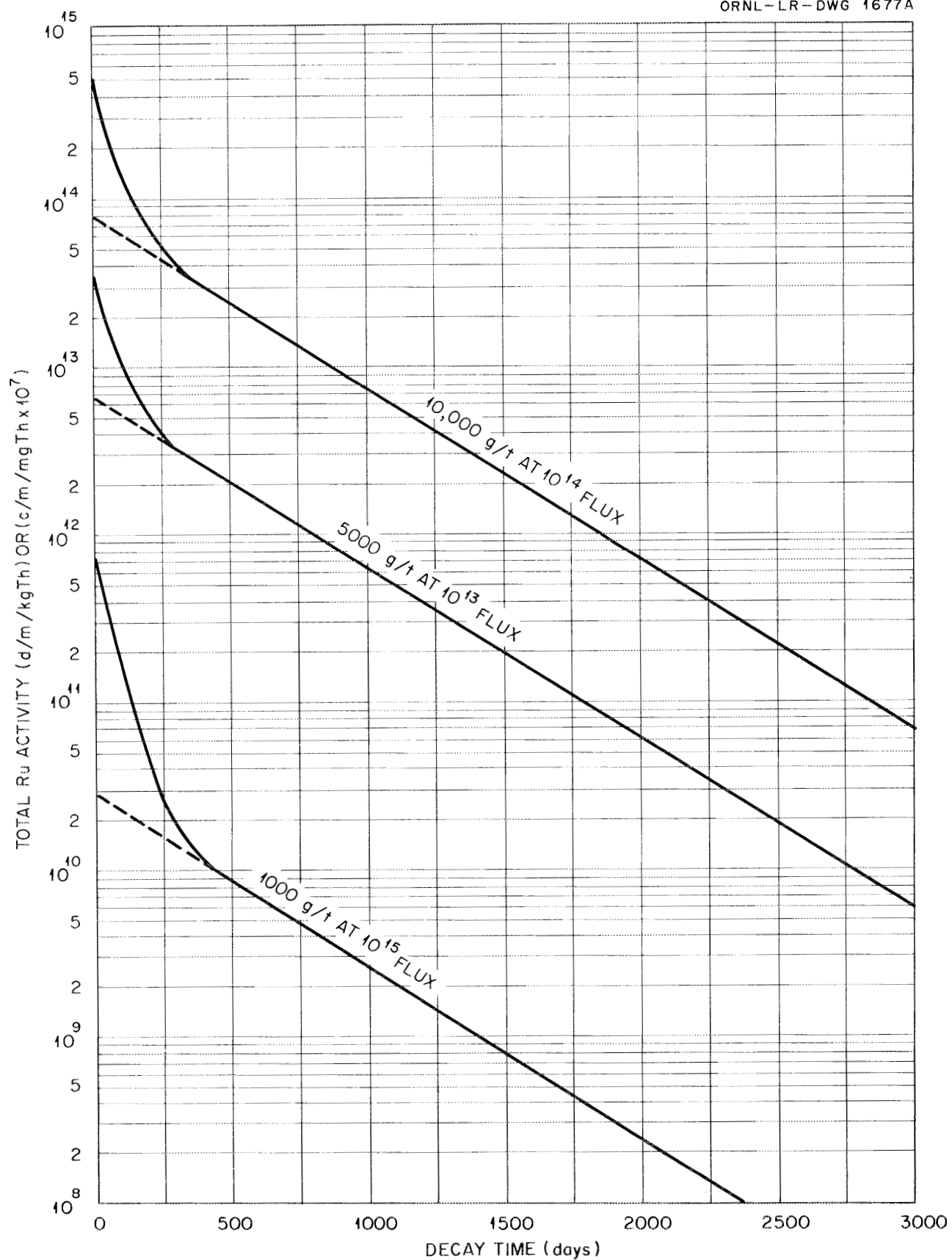


Fig. 29. Effect of Decay Time on Total Ru Activity.

Table 10. Ba^{140} and La^{140} Activities at Time of Discharge

g Mass 233 per ton Th ²³²	Blanket Processing Rate (reactor vol/day)	Ba^{140} (curies/mole Th)	La^{140} (curies/mole Th)
At Flux of 10^{13} n/cm ² /sec			
1,000	5.66×10^{-3}	3.464	3.417
2,000	2.59×10^{-3}	8.082	8.033
3,000	1.57×10^{-3}	12.802	12.756
4,000	1.05×10^{-3}	17.555	17.514
5,000	7.5×10^{-4}	22.317	22.281
7,000	3.9×10^{-4}	31.868	31.844
10,000	1.3×10^{-4}	46.204	46.199
At Flux of 5×10^{13} n/cm ² /sec			
1,000	2.893×10^{-2}	6.961	6.506
2,000	1.329×10^{-2}	23.456	22.729
3,000	8.23×10^{-3}	43.608	42.763
4,000	5.60×10^{-3}	65.476	64.613
5,000	4.01×10^{-3}	88.177	87.346
7,000	2.19×10^{-3}	135.10	134.42
10,000	8.20×10^{-4}	207.22	206.85

Table 10 (continued)

g Mass 233 per ton Th ²³²	Blanket Processing Rate (reactor vol/day)	Ba ¹⁴⁰ (curies/mole Th)	La ¹⁴⁰ (curies/mole Th)
At Flux of 10^{14} n/cm ² /sec			
1,000	5.843×10^{-2}	6.597	5.780
2,000	2.752×10^{-2}	27.821	26.087
3,000	1.705×10^{-2}	58.352	56.047
4,000	1.175×10^{-2}	94.570	91.969
5,000	8.53×10^{-3}	134.48	131.78
7,000	4.82×10^{-3}	221.12	218.61
10,000	1.99×10^{-3}	360.64	358.98
At Flux of 5×10^{14} n/cm ² /sec			
1,000	29.59×10^{-2}	2.741	1.596
2,000	14.30×10^{-2}	17.387	12.911
3,000	9.158×10^{-2}	48.132	39.388
4,000	6.555×10^{-2}	95.618	82.508
5,000	4.975×10^{-2}	159.41	142.25
7,000	3.136×10^{-2}	331.84	308.40
10,000	1.717×10^{-2}	687.55	660.08
At Flux of 10^{15} n/cm ² /sec			
1,000	59.31×10^{-2}	1.540	0.632
2,000	28.83×10^{-2}	10.714	6.306
3,000	18.61×10^{-2}	31.873	21.964
4,000	13.46×10^{-2}	67.285	50.732
5,000	10.35×10^{-2}	118.37	94.625
7,000	6.746×10^{-2}	268.51	230.77
10,000	3.989×10^{-2}	621.20	566.43

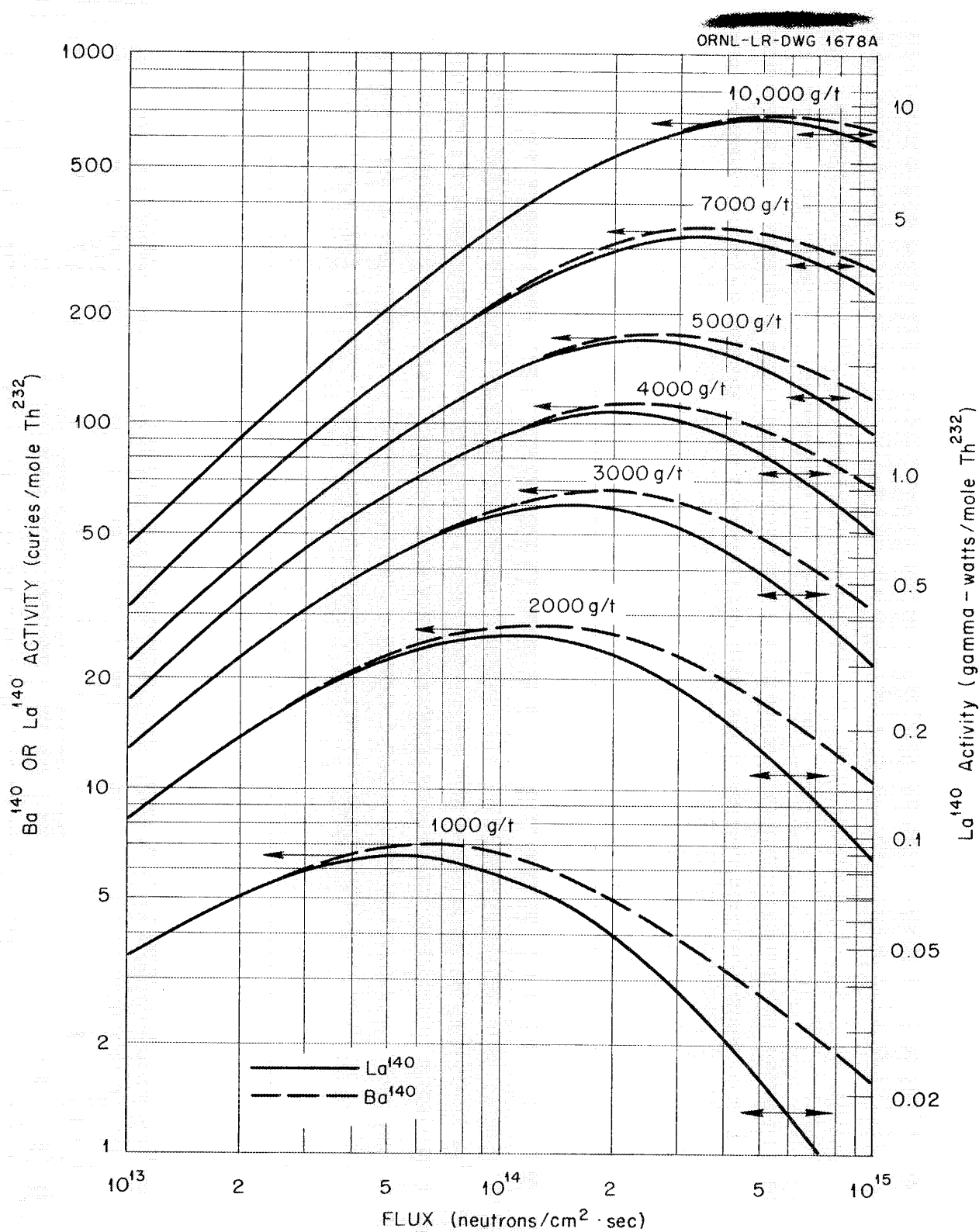


Fig. 30. Effect of Flux and g/t Level on Ba^{140} and La^{140} Activity at Time of Discharge. Arrows point to scale used.

ORNL-LR-DWG 1679A

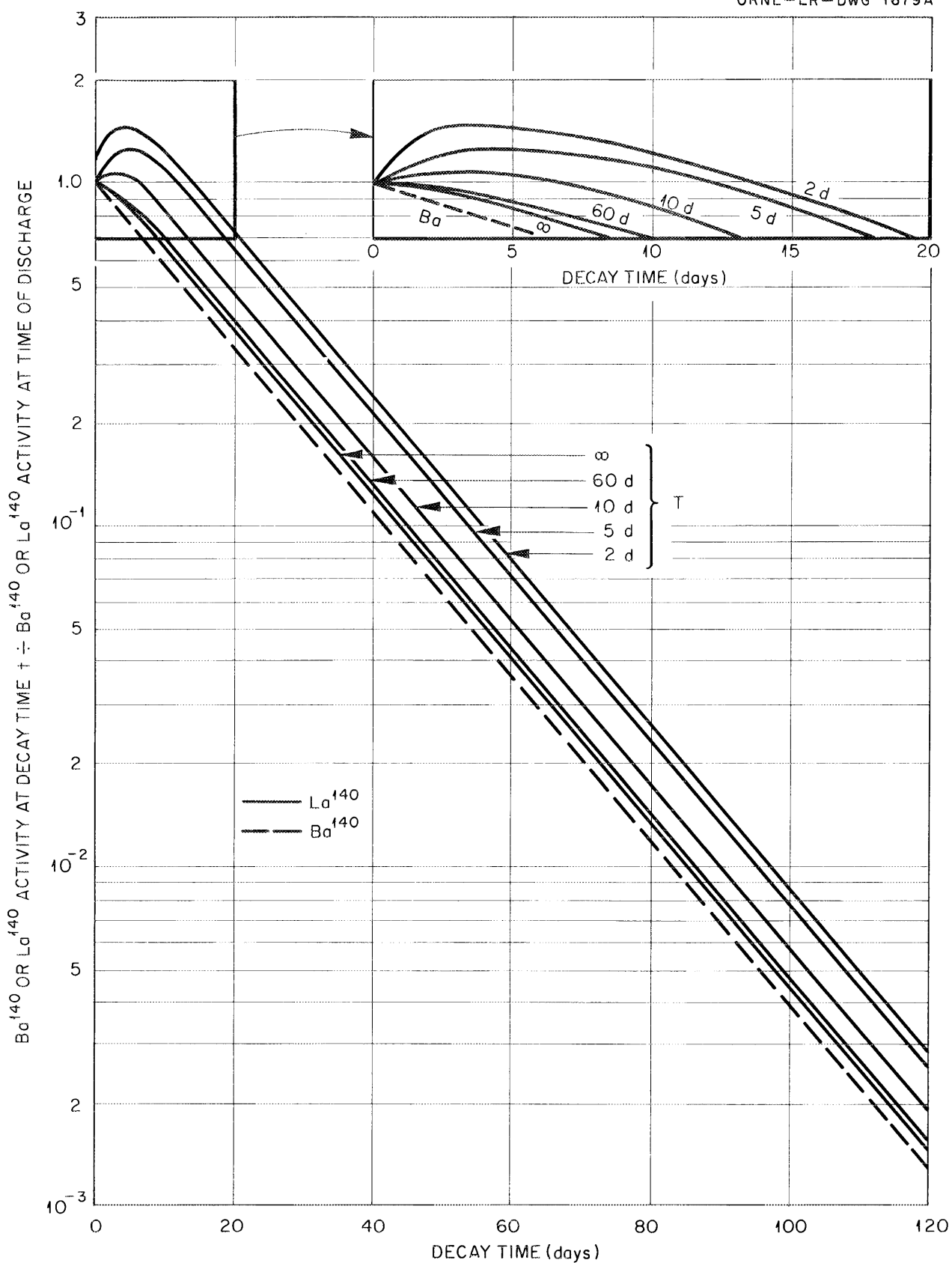


Fig. 31. Effect of Decay Time on Ba^{140} or La^{140} Activities

7.0 CALCULATIONS OF IRRADIATION PRODUCT CONCENTRATIONS

All calculations were based upon equilibrium conditions in which the rate of change of concentration with time is equal to zero. The differential equations take into consideration the formation of product "A" from "A-1" by either radioactive decay or neutron capture, burnout, or decay by product "A" and chemical processing for removal of "A". All calculations were based on irradiating 1 mole of thorium, which was assumed to be kept constant. Calculations were based on thermal flux and thermal cross sections for all materials except, of course, the $(n,2n)$ reaction on Th^{232} , and no correction was made for resonance since resonance absorption varies with the type of reactor. The term $\overline{\phi \sigma_{02}}$ is given in the equations as a correction factor applied to ϕ to include resonance absorption in Th^{232} and should be used when greater accuracy is desired.

For Pa^{233} concentration,

$$\frac{dN_{13}}{dt} = N_{02} \overline{\phi \sigma_{02}} - \overline{\phi} N_{13} \sigma_{13} - N_{13} \lambda_{13} - N_{13} C = 0 \quad (1)$$

$$N_{13} = \frac{\overline{\phi \sigma_{02}} N_{02}}{\overline{\phi \sigma_{13}} + \lambda_{13} + C} \quad (2)$$

For U^{233} concentration,

$$\frac{dN_{23}}{dt} = N_{13} \lambda_{13} - N_{23} \overline{\phi \sigma'_{23}} - N_{23} C = 0 \quad (3)$$

$$\frac{N_{23}}{N_{02}} = \frac{\overline{\phi \sigma_{02}} \lambda_{13}}{(\overline{\phi \sigma_{13}} + \lambda_{13} + C)(\overline{\phi \sigma'_{23}} + C)} \quad (4)$$

$$\frac{dN_{24}}{dt} = N_{23} \phi \sigma_{23} + N_{13} \phi \sigma_{13} - N_{24} \phi \sigma_{24} - N_{24} C = 0 \quad (5)$$

$$N_{24} = \frac{N_{23} \phi \sigma_{23} + N_{13} \phi \sigma_{13}}{\phi \sigma_{24} + C} \quad (6)$$

$$\frac{N_{24}}{N_{02}} = \frac{\frac{N_{23}}{N_{02}} \phi \sigma_{23} + \frac{N_{13}}{N_{02}} \phi \sigma_{13}}{\phi \sigma_{24} + C} \quad (7)$$

or

$$\frac{N_{24}}{N_{02}} = \frac{\overline{\phi \sigma_{02}} \overline{\phi \sigma_{23}} \lambda_{13} + (\overline{\phi \sigma_{02}} \overline{\phi \sigma_{13}})(\phi \sigma'_{23} + C)}{(\phi \sigma_{13} + \lambda_{13} + C)(\phi \sigma'_{23} + C)(\phi \sigma_{24} + C)} \quad (8)$$

For U^{235} concentration,

$$\frac{dN_{25}}{dt} = N_{24} \phi \sigma_{24} - N_{25} \phi \sigma_{25} - N_{25} C = 0 \quad (9)$$

$$\frac{N_{25}}{N_{24}} = \frac{\sigma_{24}}{\sigma'_{25} + C/\phi} = \frac{\phi \sigma_{24}}{\phi \sigma'_{25} + C} \quad (10)$$

$$\frac{N_{25}}{N_{02}} = \frac{\overline{\phi \sigma_{02}} \phi^2 \lambda_{13} \sigma_{23} \sigma_{24} + \overline{\phi \sigma_{02}} \phi^2 \sigma_{24} \sigma_{13} \phi (\sigma'_{23} + C)}{(\phi \sigma'_{25} + C)(\phi \sigma_{13} + \lambda_{13} + C)(\phi \sigma'_{23} + C)(\phi \sigma_{24} + C)} \quad (11)$$

For Th^{234} concentration,

$$\frac{dN_{04}}{dt} = N_{03} \phi \sigma_{03} - N_{04} \lambda_{04} - N_{04} C = 0 \quad (12)$$

$$\frac{dN_{03}}{dt} = N_{02} \overline{\phi \sigma_{02}} - N_{03} \lambda_{03} - \phi N_{03} \sigma_{03} - N_{03} C = 0 \quad (13)$$

$$\frac{N_{03}}{N_{02}} = \frac{\overline{\phi} \sigma_{02}}{\lambda_{03} + \overline{\phi} \sigma_{03} + c} \quad (14)$$

$$\frac{N_{04}}{N_{03}} = \frac{\overline{\phi} \sigma_{03}}{\lambda_{04} + c} \quad (15)$$

$$\frac{N_{04}}{N_{02}} = \frac{\overline{\phi} \sigma_{02} \overline{\phi} \sigma_{03}}{(\lambda_{03} + \overline{\phi} \sigma_{03} + c)(\lambda_{04} + c)} \quad (16)$$

For fission product concentrations,

$$\frac{dN_{FP}}{dt} = 2\overline{\phi} N_{23} \sigma_{f23} - N_{FP} C = 0 \quad (17)$$

$$\frac{N_{FP}}{N_{23}} = \frac{2\overline{\phi} \sigma_{f23}}{C} \quad (18)$$

$$\frac{N_{FP}}{N_{02}} = \frac{2\overline{\phi} \sigma_{f23}}{C} \frac{\overline{\phi} \sigma_{02} \lambda_{13}}{(\sigma_{13} \overline{\phi} + \lambda_{13} + c)(\overline{\phi} \sigma_{23}^l + c)} \quad (19)$$

or

$$\frac{N_{FP}}{N_{02}} = \frac{2\overline{\phi} \sigma_{f23} \lambda_{13} \overline{\phi} \sigma_{02}}{c(\overline{\phi} \sigma_{13} + \lambda_{13} + c)(\overline{\phi} \sigma_{23}^l + c)} \quad (20)$$

For fission product activities,

$$A_{FP} = \lambda N_{FP} \quad (21)$$

$$\frac{dN_{FP}}{dt} = \phi \sum_f y_f - N_{FP} \lambda_{FP} - N_{FP} C = 0 \quad (22)$$

$$N_{FP} = \phi \sum_f y / (\lambda + C) \quad (23)$$

where $\sum_f = \frac{N_{23}}{N_{02}} \times 0.602 \times 10^{24} \sigma_{f23} \text{ cm}^2/\text{mole Th}$

For the activity of ruthenium,

$$A_{Ru} = \frac{\phi \sum_f y \cdot \lambda_{Ru}}{\lambda_{Ru} + C} \text{ per mole of Th or } \frac{\phi \sum_f y \lambda_{Ru}}{\lambda_{Ru} + C} \times \frac{1000}{232} \text{ per kilogram of Th (24)}$$

where $y_{Ru}^{106} = 0.235 \times 10^{-2}\%$, $y_{Ru}^{103} = 0.93 \times 10^{-2}\%$

For barium activity,

$$A_{Ba} = \frac{\phi \sum_f y \lambda_{Ba}}{\lambda_{Ba} + C} \quad (25)$$

But for lanthanum activity,

$$\frac{dN_{La}}{dt} = N_{Ba} \lambda_{Ba} - N_{La} \lambda_{La} - N_{La} C = 0 \quad (26)$$

$$N_{La} = \frac{N_{Ba} \lambda_{Ba}}{\lambda_{La} + C} = \frac{\phi \sum_f y \lambda_{Ba}}{(\lambda_{Ba} + C)(\lambda_{La} + C)} \quad (27)$$

$$A_{La} = N_{La} \lambda_{La} = \frac{\phi \sum_f y \lambda_{Ba} \lambda_{La}}{(\lambda_{Ba} + C)(\lambda_{La} + C)} \quad (28)$$

where $y = 5.8\%$. For the activities of barium and lanthanum at various decay periods,

$$A_{Ba}(t) = A_{Ba}(\text{ATD}) e^{-\lambda_{Ba} t} \quad (29)$$

$$A_{La}(t) = A_{Ba}(\text{ATD}) \frac{\lambda_{La} (e^{-\lambda_{Ba} t} - e^{-\lambda_{La} t})}{\lambda_{La} - \lambda_{Ba}} + A_{La}(\text{ATD}) e^{-\lambda_{La} t} \quad (30)$$

For the processing rate, which is the reciprocal of the processing period, based on the g/t level, a new term, G, i.e., atoms of $\text{Pa}^{233} + \text{U}^{233}$ per atom of Th^{232} , is defined:

$$G = \frac{N_{13} + N_{23}}{N_{02}} = g/t \times 10^{-6} \times \frac{232}{233} = 9.99 \times 10^{-7} \text{ g/t} \quad (31)$$

$$G = \frac{\overline{\phi \sigma_{02}}}{\overline{\phi \sigma_{13}} + \lambda_{13} + C} + \frac{\overline{\phi \sigma_{02}} \lambda_{13}}{(\overline{\phi \sigma_{13}} + \lambda_{13} + C)(\overline{\phi \sigma_{23}^l} + C)} \quad (32)$$

$$G \left[(\overline{\phi \sigma_{13}} + \lambda_{13}) \overline{\phi \sigma_{23}^l} + (\overline{\phi \sigma_{13}} + \lambda_{13}) C + \overline{\phi \sigma_{23}^l} C + C^2 \right] = \overline{\phi \sigma_{02}} \overline{\phi \sigma_{23}^l} + \overline{\phi \sigma_{02}} \lambda_{13} + \overline{\phi \sigma_{02}} C \quad (33)$$

$$CG(\overline{\phi \sigma_{13}} + \lambda_{13} + \overline{\phi \sigma_{23}^l} - \frac{\overline{\phi \sigma_{02}}}{G}) + C^2 G =$$

$$\overline{\phi \sigma_{02}} \overline{\phi \sigma_{23}^l} + \overline{\phi \sigma_{02}} \lambda_{13} - G \overline{\phi \sigma_{23}^l} (\overline{\phi \sigma_{13}} + \lambda_{13}) \quad (34)$$

$$\text{Let } A = (\overline{\phi \sigma_{13}} \lambda_{13} + \overline{\phi \sigma_{23}^l} - \frac{\overline{\phi \sigma_{02}}}{G}) G \quad (35)$$

$$B = \overline{\phi \sigma_{02}} \overline{\phi \sigma_{23}^l} + \overline{\phi \sigma_{02}} \lambda_{13} - G \overline{\phi \sigma_{23}^l} (\overline{\phi \sigma_{13}} + \lambda_{13}) \quad (36)$$

then

$$AC + C^2 G = B \quad (37)$$

$$C = \frac{-A + \sqrt{A^2 + 4BG}}{2G} \quad (38)$$

The negative radical term is not used since it always gives a physically impossible root.

8.0 CONSTANTS AND DEFINITIONS OF SYMBOLS

The following symbols are used in this report:

N^o	= initial concentration of given nuclide
N	= concentration of given nuclide
ϕ	= flux ($n/cm^2/sec$)
t	= time (sec)
y	= fission yield of given fission product
T	= processing period (days)
A^o	= activity at time of reactor discharge
C	= chemical processing rate in reciprocal days (see Eq. 38)
g/t	= grams of $U^{233} + Pa^{233}$ per ton of Th^{232}
λ	= decay constant of a given nuclide
γ	= flux-period product = $\phi T \times 10^{-14} n\text{-days}/cm^2 \cdot sec$
$_{02}$	= Th^{232}
$_{04}$	= Th^{234}
$_{11}$	= Pa^{231}
$_{13}$	= Pa^{233}
$_{22}$	= U^{232}
$_{23}$	= U^{233}
$_{24}$	= U^{234}
$_{25}$	= U^{235}
$_{26}$	= U^{236}
$_{27}$	= U^{237}
FP	= fission products

Table 13. Cross-section Values

Symbol	Value (barns)	Symbol	Value (barns)
Capture		Absorption	
σ_{02}	7	σ'_{23}	560
σ_{03}	1350	σ'_{25}	640
σ_{11}	250	Fission	
σ_{13}	150	σ_{f23}	505
σ_{23}	55	σ_{f25}	540
σ_{24}	70	Reaction	
σ_{25}	100	$\sigma_{02}(n,2n)$	0.002- 0.013
σ_{26}	20		

Table 14. Half-life Values

Nuclide	Type of Emission and Energy (Mev)	Half-life
^{231}Th	β^- 0.3, 0.22, 0.09; γ 0.022-0.21	25.5h
^{232}Th	α 4.03	1.39×10^{10} y
^{233}Th	β^- 1.23	23.5m
^{234}Th	β^- 0.2, 0.11; γ 0.093	24.1d
^{232}Pa	β^- 0.33; γ 0.05 - 0.96	1.32d
^{233}Pa	β^- 0.58, 0.48, 0.27; γ 0.1, 0.31	27.4d
$^{234}\text{Pa}^a$	β^- 2.3; γ 0.8	1.14m
^{232}U	α 5.31	70y
^{233}U	α 4.82	1.62×10^5 y
^{234}U	α 4.76	2.6×10^5 y
^{235}U	α 4.2 - 4.6	7.1×10^8 y
^{237}U	β^- 0.23; γ 0.2; 0.06, 0.26	6.7d
^{103}Ru	β^- 0.217; γ 0.498	40d
^{106}Ru	β^- 0.038	290d

^a Pa^{234} as UZ with a 6.7h half-life was not considered. The Pa^{234} was assumed to be UX₂ whether formed by Th^{234} decay or a $\text{Pa}^{233}(n,\gamma)$ reaction.

Table 15. Decay Constant Values

Symbol	Value
λ_{08}	$3.647 \times 10^{-1} \text{y}^{-1}$
λ_{22}	$9.9 \times 10^{-3} \text{y}^{-1}$
λ_{23}	$4.28 \times 10^{-6} \text{y}^{-1}$
$\lambda_{\text{Ru}^{103}}$	$1.2 \times 10^{-5} \text{m}^{-1}$ or $1.733 \times 10^{-3} \text{d}^{-1}$
$\lambda_{\text{Ru}^{106}}$	$1.66 \times 10^{-6} \text{m}^{-1}$ or $2.389 \times 10^{-3} \text{d}^{-1}$

9.0 REFERENCES

1. R. W. Stoughton, D. E. Ferguson, J. Halperin, and C. V. Ellison, ORNL-1462 (May 5, 1953)
2. P. Fields, E. Gerngross, and H. Diamond, ANL-4861 (February 1, 1952)
3. E. K. Hyde, R. J. Bruehlman, and W. M. Manning, ANL-4165 (June 25, 1948)
4. E. D. Arnold and A. T. Gresky, ORNL 1818 (December 5, 1955)
5. R. W. Stoughton and J. Halperin ORNL, letter to F. L. Culler, ORNL (January, 1954)